Colloid stability, DLVO and dynamic light scattering
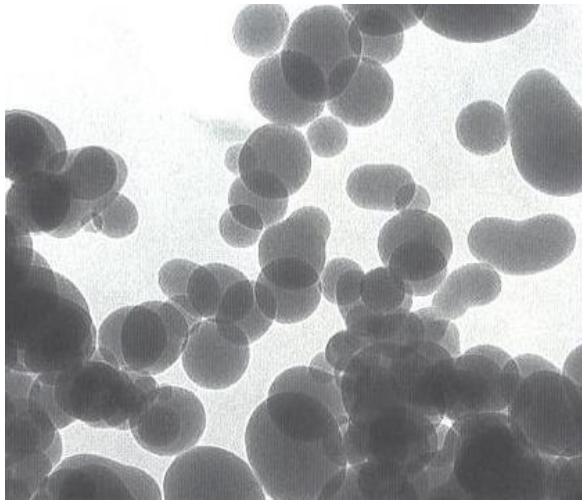
Ana Maria Carmona-Ribeiro

amcr@usp.br

Biocolloids Lab
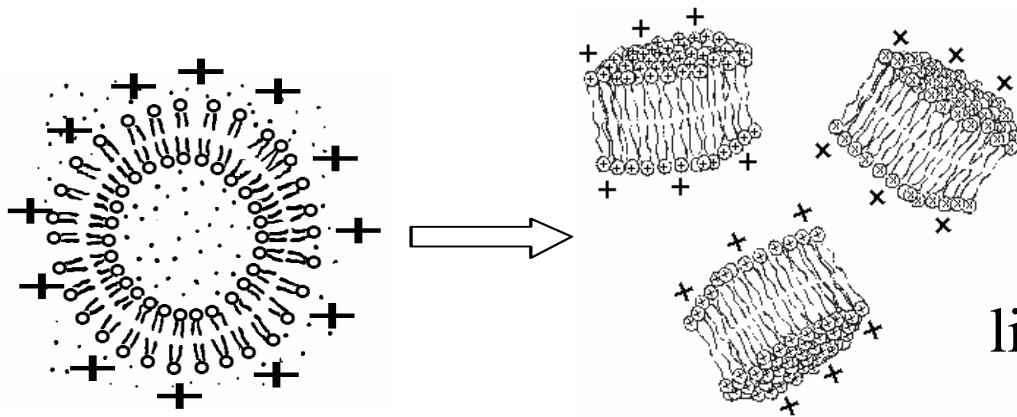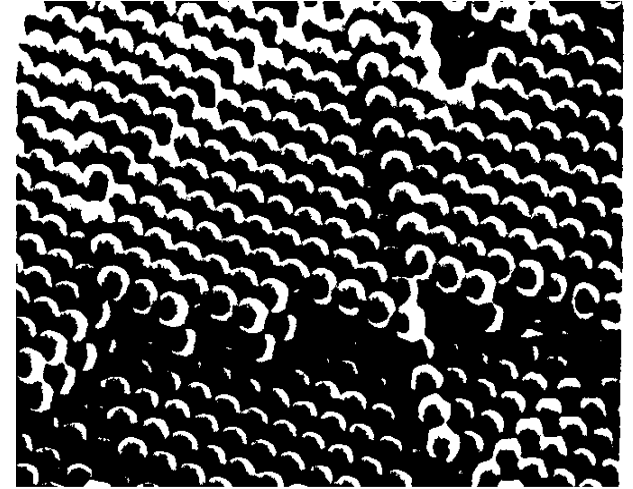
Universidade de São Paulo

Colloids: particles and association colloids

latex

silica

lipid bilayer fragments

COLOIDES DE ASSOCIAÇÃO

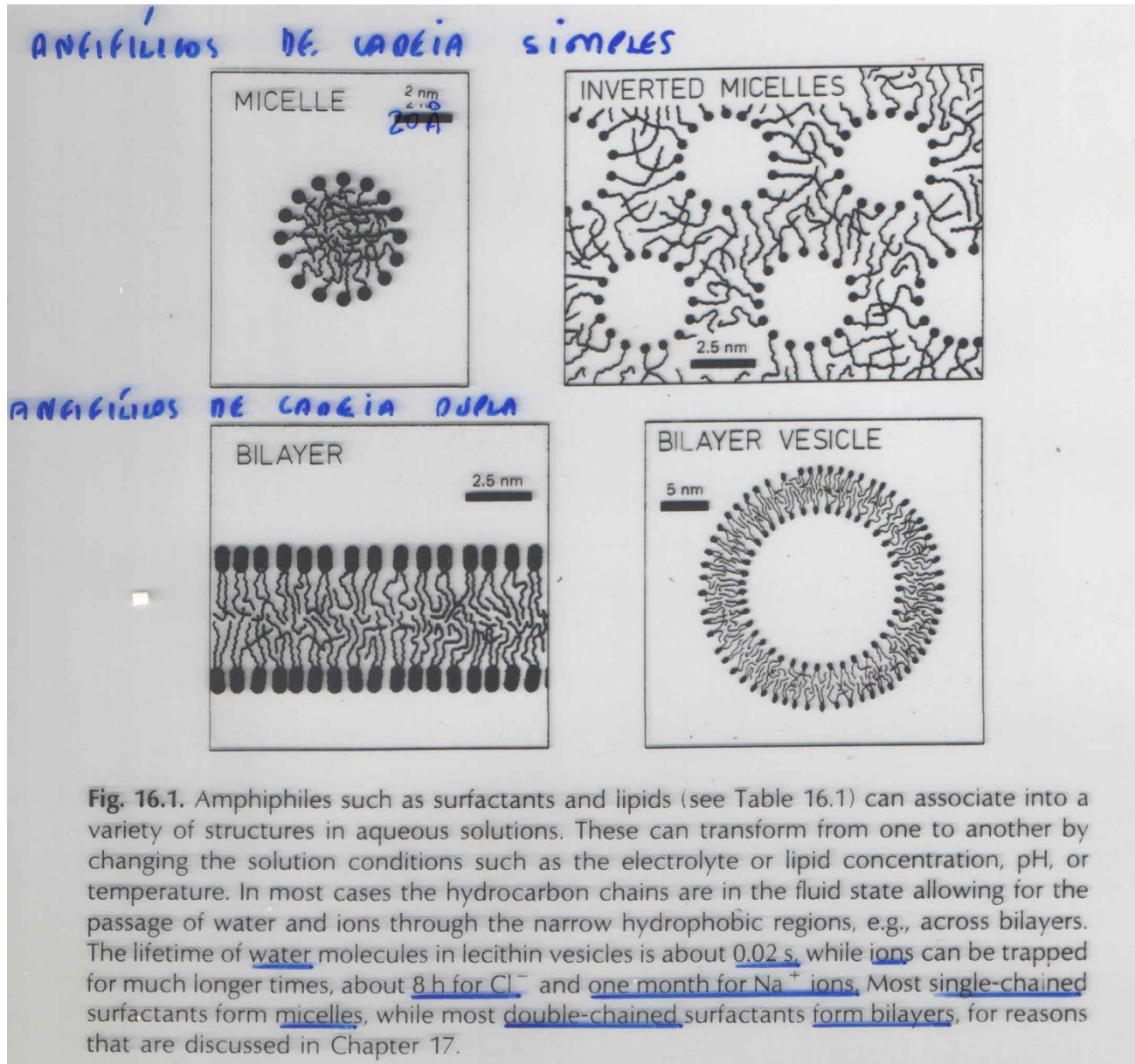Autoassociação de moléculas anfifílicas.
Agregados supramoleculares e geometria molecular.
Micelas, monocamadas, bicamadas, vesículas, lipossomos e membranas celulares.
Biomembranas.
Forças de interação intra- e interagregados (eletrostática, van der Waals, hidrofóbica, solvatação).
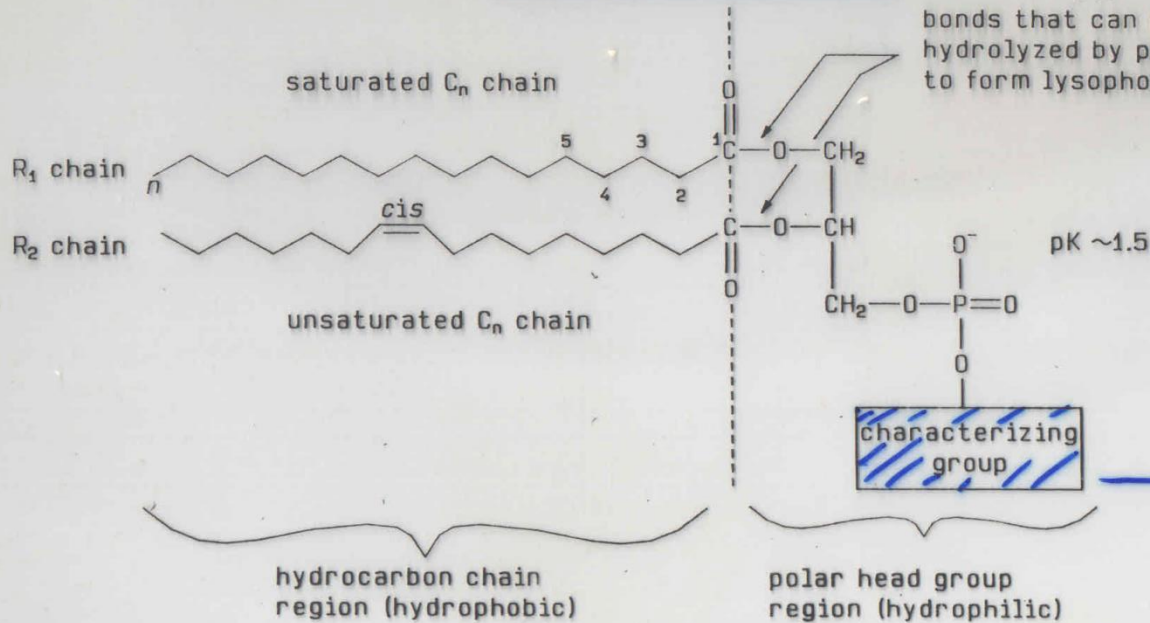
Autoassociação de moléculas anfifílicas

ANFIFÍLICOS DE CADEIA SIMPLES

ANFIFÍLICOS DE CADEIA DUPLA

Fig. 16.1. Amphiphiles such as surfactants and lipids (see Table 16.1) can associate into a variety of structures in aqueous solutions. These can transform from one to another by changing the solution conditions such as the electrolyte or lipid concentration, pH, or temperature. In most cases the hydrocarbon chains are in the fluid state allowing for the passage of water and ions through the narrow hydrophobic regions, e.g., across bilayers. The lifetime of water molecules in lecithin vesicles is about 0.02 s, while ions can be trapped for much longer times, about 8 h for Cl^- and one month for Na^+ ions. Most single-chained surfactants form micelles, while most double-chained surfactants form bilayers, for reasons that are discussed in Chapter 17.

Anionic	$C_{12}H_{25}$—O-SO_3^- Na^+	Sodium dodecyl sulphate (SDS or NaDS)
Anionic	$C_{18}H_{37}$—COO^- H^+	Stearic acid
Cationic	$C_{16}H_{33}$—$N^+(CH_3)_3 Br^-$	Hexadecyl trimethylammonium bromide (HTAB or CTAB)
Non-ionic	$C_{12}H_{25}$—$(O-CH_2-CH_2)_5$-OH	Pentaoxyethylene dodecyl ether ($C_{12}E_5$)
Zwitterionic	Single chained lecithin (see below)	Lysolecithin

Double-chained phospholipids

saturated C_n chain

bonds that can be hydrolyzed by phospholipases to form lysophospholipids

R_1 chain

R_2 chain

cis

unsaturated C_n chain

pK ~1.5

FOSFATIDIL COM CARGA NEGATIVA

characterizing group

hydrocarbon chain region (hydrophobic)

polar head group region (hydrophilic)

Hydrocarbon chains[a]	Name of phospholipid[b]	Characterizing group[c]	
Normally contain 16–18 carbons per chain, the R_2 chain containing 1–3 cis	...phosphatidic acid (anionic)	—H	pK ~ 11
diC_{12}: dilauroyl...	...phosphatidyl choline or lecithin (zwitterionic)	—CH_2—CH_2—$N^+(CH_3)_3$	
diC_{14}: dimyristoyl...	...phosphatidyl ethanolamine (zwitterionic)	—CH_2—CH_2—NH_3^+ pK ~ 11	
diC_{16}: dipalmitoyl...	...phosphatidyl glycerol (anionic)	—CH_2—CH (with CH_2OH and OH)	

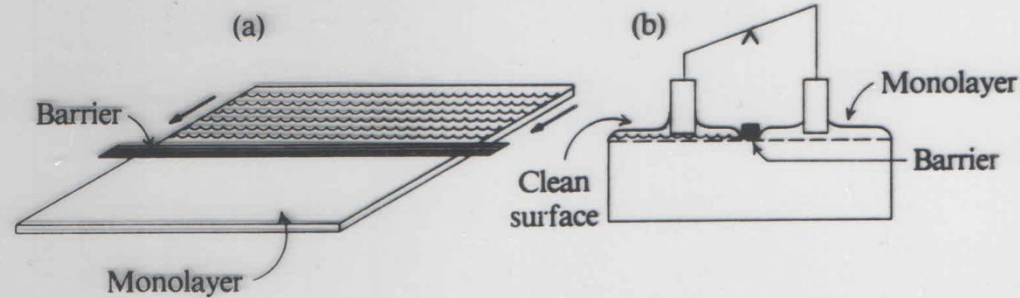# Agregação na interface ar/água: anfifílicos em monocamadas

Figure 7.1 (a) Schematic illustration of a barrier delineating the area of a monolayer and (b) a Wilhelmy plate arrangement for measuring the difference in γ on opposite sides of barrier.
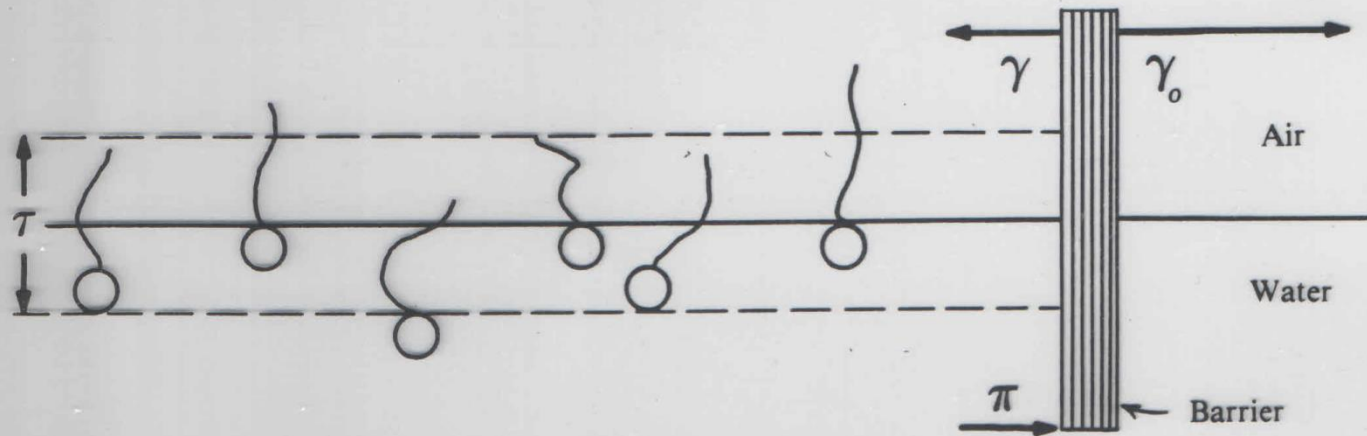

Figure 7.2 Schematic profile of the air–water interface at a barrier which separates a monolayer from the clean surface.
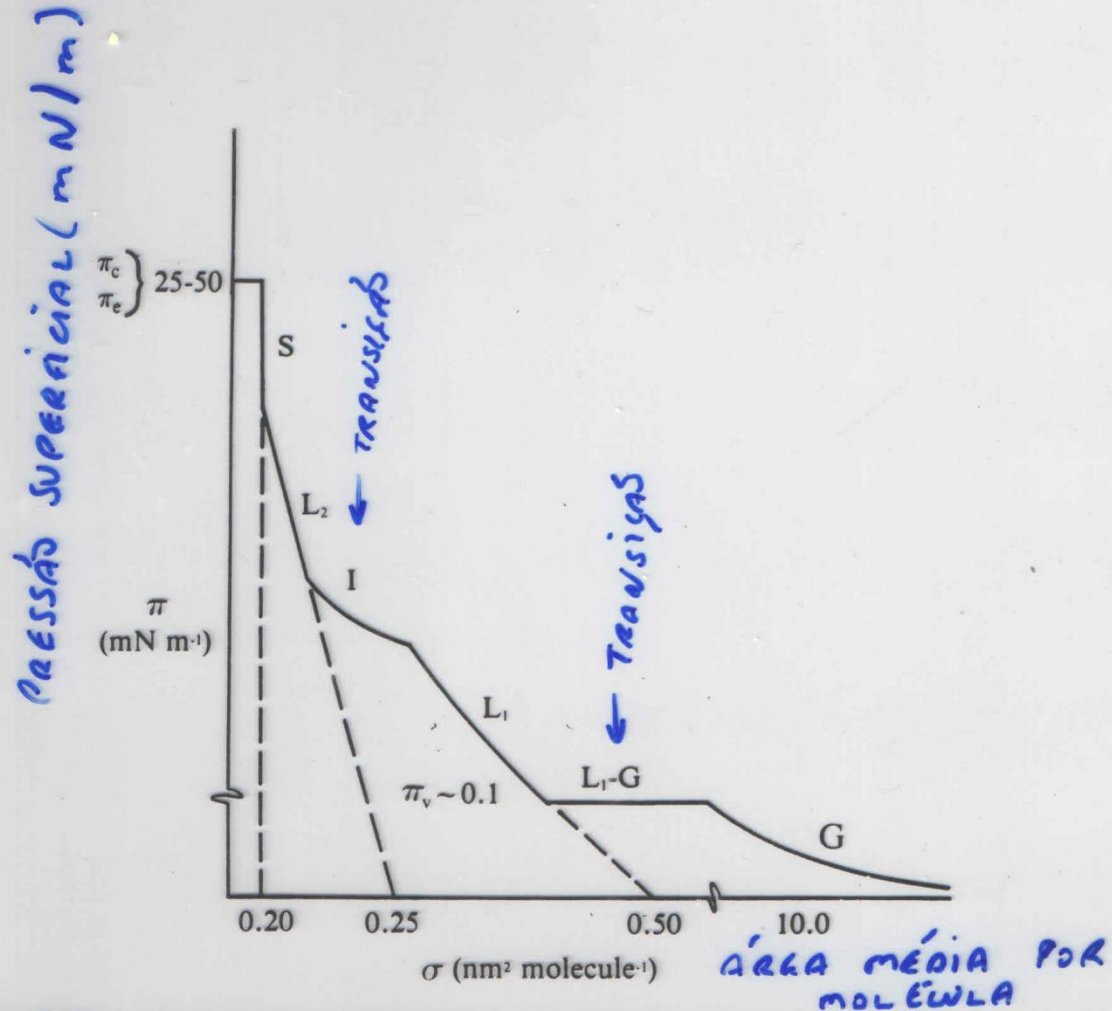
Isoterma Pressão/Área por molécula

Figure 7.5 Composite two-dimensional pressure (π)–area (σ) isotherm which includes a wide assortment of monolayer phenomena. Note that the scale of the figure is not uniform so that all features may be included on one set of coordinates.

Deposição de filmes em superfícies sólidas (filmes de Langmuir-Blodgett)

SOLID COATED
WITH FIRST
LAYER

ar

água
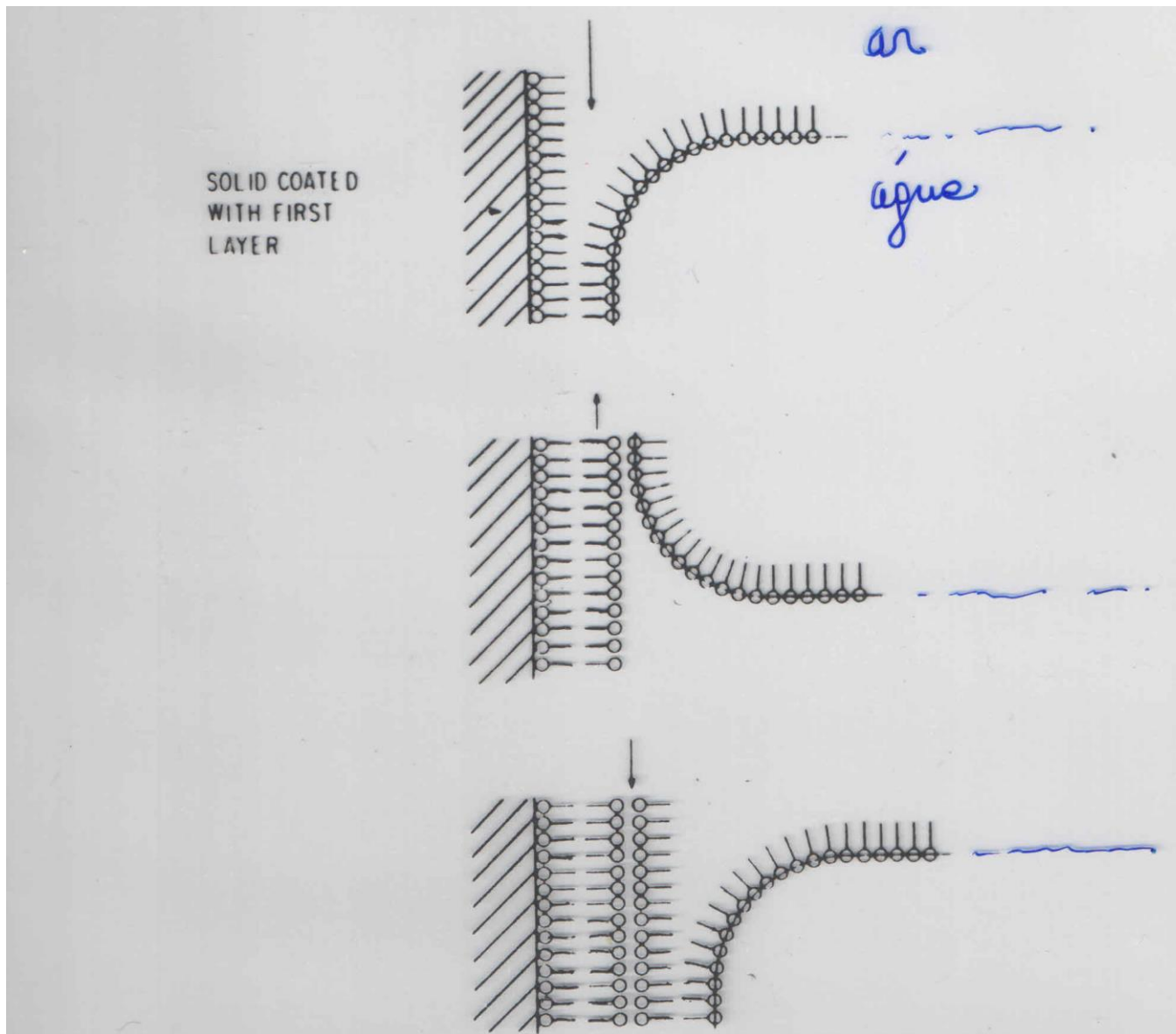
Figure D.6 The building up of a Langmuir Blodgett film (Gaines, 1966, p. 337).

FATORES QUE GOVERNAM A AUTOASSOCIAÇÃO

- ## FATORES TERMODINÂMICOS:

- POTENCIAL QUÍMICO PADRÃO μ_N^0 PARA UMA MOLÉCULA NO ESTADO AGREGADO É MENOR QUE μ_A^0 (MOLÉCULA NÃO-AGREGADA)

$$\mu_N^0 < \mu_A^0$$
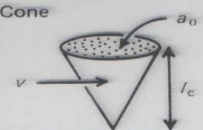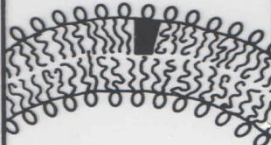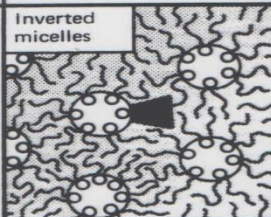
- ## FORÇAS DE INTERAÇÃO INTRA-AGREGADOS:

- ATRAÇÃO E REPULSÃO INTER MOLÉCULAS FORÇAS INTERMOLECULARES

- ## GEOMETRIA MOLECULAR:

- COMPRIMENTO DA(S) CADEIA(S) HIDROCARBÔNICA) ℓ

- VOLUME DA(S) CADEIA(S) HIDROCARBÔNICA ν

- ÁREA DA CABEÇA POLAR a

TABLE 17.2 Mean (dynamic) packing shapes of lipids and the structures they form

Lipid	Critical packing parameter $v/a_0 l_c$	Critical packing shape GEOMETRIA	Structures formed AGREGADO
Single-chained lipids (surfactants) with large head-group areas: *SDS in low salt*	< 1/3	Cone	Spherical micelles
Single-chained lipids with small head-group areas: *SDS and CTAB in high salt, nonionic lipids*	1/3–1/2	Truncated cone	Cylindrical micelles
Double-chained lipids with large head-group areas, fluid chains: *Phosphatidyl choline (lecithin), phosphatidyl serine, phosphatidyl glycerol, phosphatidyl inositol, phosphatidic acid, sphingomyelin, DGDG[a], dihexadecyl phosphate, dialkyl dimethyl ammonium salts*	1/2–1	Truncated cone	Flexible bilayers, vesicles
Double-chained lipids with small head-group areas, anionic lipids in high salt, saturated frozen chains: *phosphatidyl ethanolamine, phosphatidyl serine + Ca^{2+}*	~1	Cylinder	Planar bilayers
Double-chained lipids with small head-group areas, nonionic lipids, poly *(cis)* unsaturated chains, high *T*: *unsat. phosphatidyl ethanolamine, cardiolipin + Ca^{2+} phosphatidic acid + Ca^{2+} cholesterol, MGDG[b]*	> 1	Inverted truncated cone or wedge	Inverted micelles

[a] DGDG, digalactosyl diglyceride, diglucosyl diglyceride.
[b] MGDG, monogalactosyl diglyceride, monoglucosyl diglyceride.

$v/(a.l)$ ↑ , TAMANHO AGREGADO ↑

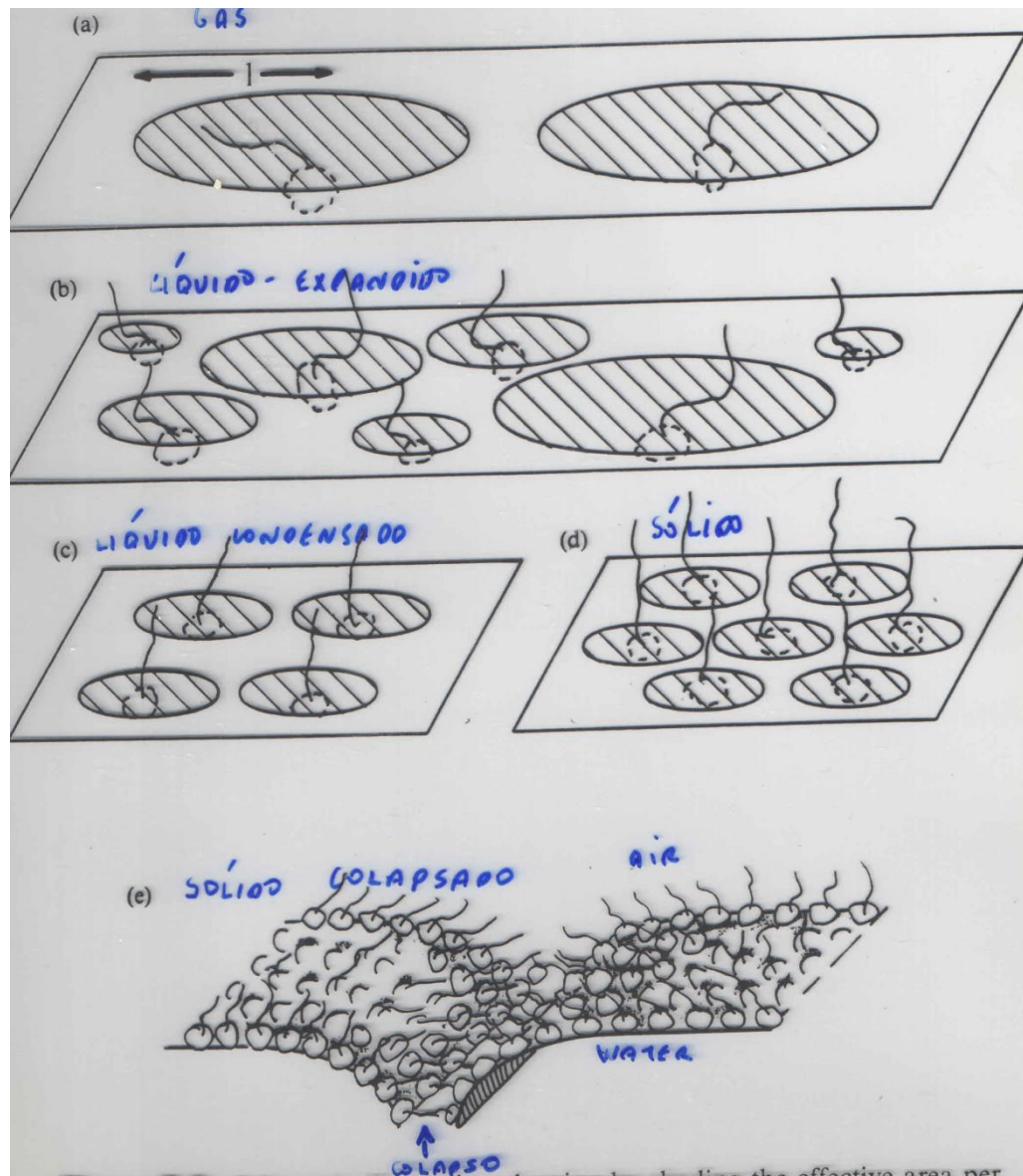# Os vários estados físicos de uma monocamada

Figure 7.6 Schematic illustration showing by shading the effective area per molecule at various stages of monolayer compression: (a) gaseous state, (b) liquid expanded state, (c) liquid condensed state, and (d) solid state. In (e) the collapse of the film is illustrated.

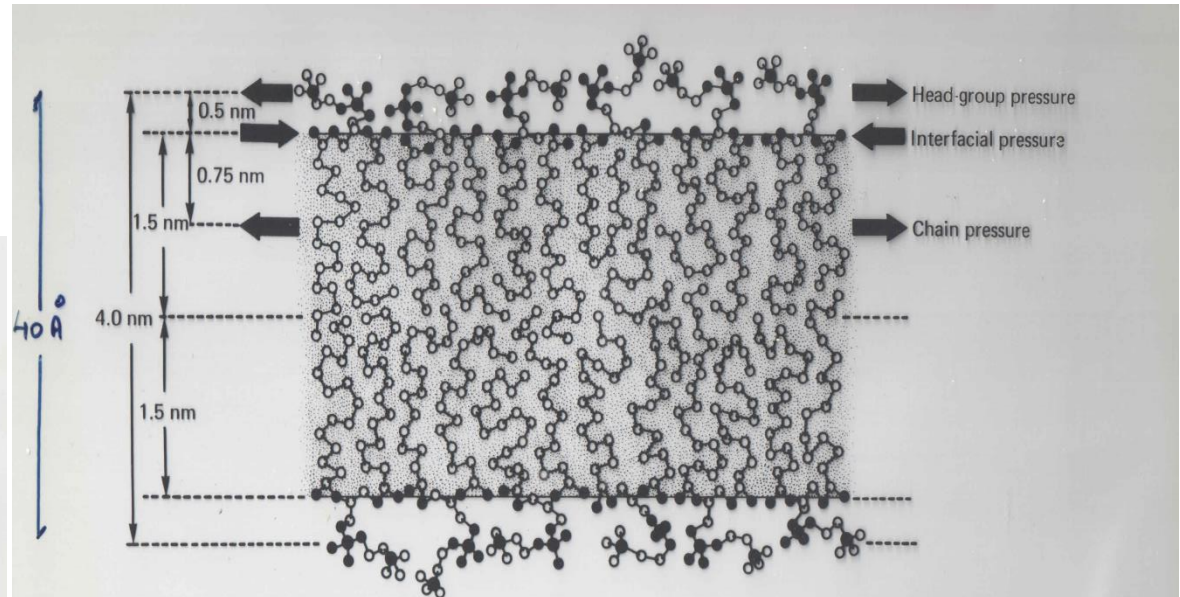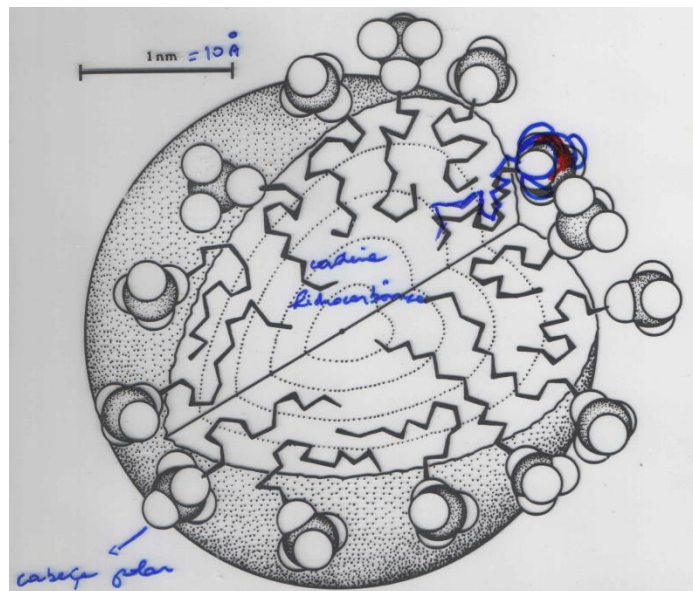# Dimensões de micela de SDS e bicamada de fosfatidilcolina

Fig. 17.4. Lecithin bilayer drawn to scale. The lipid bilayer is the basic structure of biological membranes, and most membrane lipids contain two hydrocarbon chains. The lipids diffuse rapidly in the plane of the bilayer, covering a distance of about 1 μm in 1 s. They also cross the bilayer from one side to the other ('flip-flop'), as well as exchange with lipids in the solution, but at much slower rates, of the order of hours (cf. the lifetime of single-chained surfactants in micelles of 10^{-5} to 10^{-3} s). (From Israelachvili et al., 1980a.)

Primeira teoria de estabilidade coloidal : DLVO

Interaction energy against separation distance between two particles:
the sum between attraction (-) and repulsion (+)
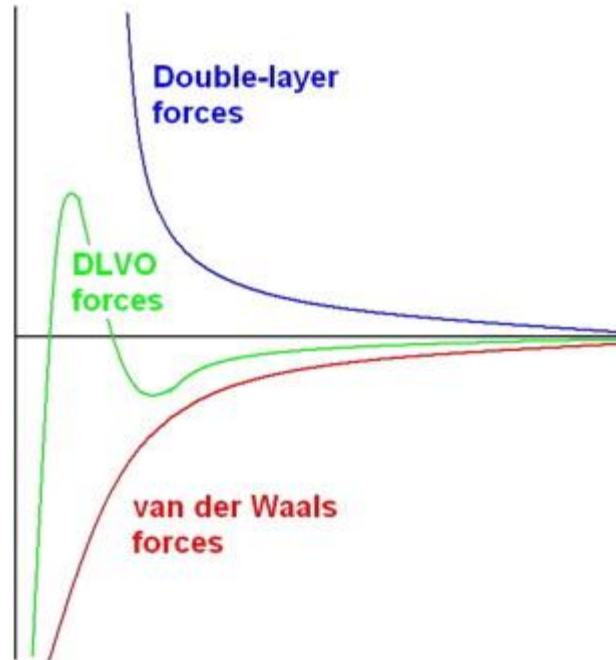
Dynamic light scattering (**photon correlation spectroscopy** or **quasi-elastic light scattering**) is a technique in [physics](#) that can be used to determine the size distribution profile of small [particles](#) in [suspension](#) or [polymers](#) in [solution](#)
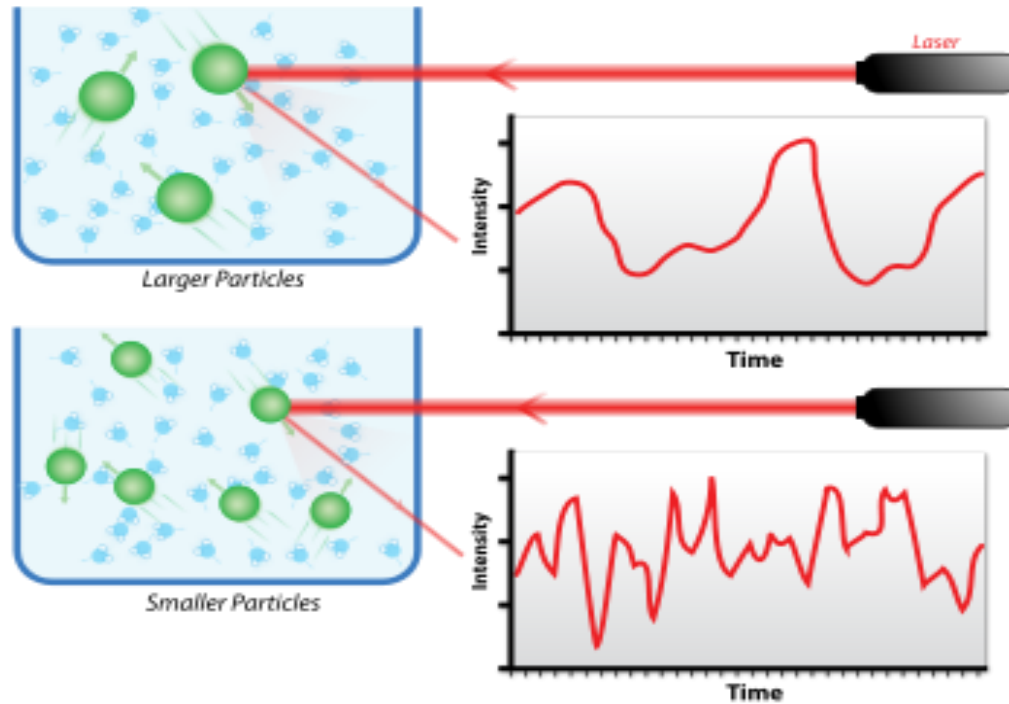
When light hits small particles, the light scatters in all directions ([Rayleigh scattering](#)) as long as the particles are small compared to the wavelength (below 250 [nm](#)). If the light source is a [laser](#), and thus is [monochromatic](#) and [coherent](#), then one observes a time-dependent fluctuation in the scattering intensity. This fluctuation is due to the fact that the small molecules in solutions are undergoing [Brownian motion](#), and so the distance between the scatterers in the solution is constantly changing with time. This scattered light then undergoes either constructive or destructive interference by the surrounding particles, and within this intensity fluctuation, information is contained about the time scale of movement of the scatterers. Sample preparation either by filtration or centrifugation is critical to remove dust and artifacts from the solution.

The dynamic information of the particles is derived from an autocorrelation of the intensity trace recorded during the experiment.

The second order autocorrelation curve is generated from the intensity trace as follows:

$$g^2(q; \tau) = \frac{\langle I(t)I(t+\tau)\rangle}{\langle I(t)\rangle^2}$$

where g is the autocorrelation function at a particular wave vector, q , and delay time, tau , and I is the intensity.

At short time delays, the correlation is high because the particles do not have a chance to move to a great extent from the initial state that they were in. The two signals are thus essentially unchanged when compared after only a very short time interval. As the time delays become longer, the correlation decays exponentially, meaning that, after a long time period has elapsed, there is no correlation between the scattered intensity of the initial and final states.

This exponential decay is related to the motion of the particles, specifically to the diffusion coefficient. To fit the decay (i.e., the autocorrelation function), numerical methods are used, based on calculations of assumed distributions. If the sample is monodisperse then the decay is simply a single exponential.

Once the autocorrelation data have been generated, different mathematical approaches can be employed to determine 'information' from it. Analysis of the scattering is facilitated when particles do not interact through collisions or electrostatic forces between ions. Particle-particle collisions can be suppressed by dilution, and charge effects are reduced by the use of salts to collapse the electrical double layer. The simplest approach is to treat the first order autocorrelation function as a single exponential decay. This is appropriate for a monodisperse population.

$$\Gamma = q^2 D_t$$

where Γ is the decay rate. The translational diffusion coefficient D_t may be derived at a single angle or at a range of angles depending on the wave vector q.

with $\qquad q = \frac{4\pi n_0}{\lambda} \sin\left(\frac{\theta}{2}\right)$

where λ is the incident laser wavelength, n_0 is the refractive index of the sample and θ is angle at which the detector is located with respect to the sample cell.

$$D = \frac{kT}{f} = \frac{kT}{6\pi\eta R_H}$$

D is often used to calculate the <u>hydrodynamic radius</u> of a sphere through the <u>Stokes–Einstein equation</u> above where k is the Boltzmann constant, T is the temperature, h is the medium viscosity, and f = 6phRH is the frictional coefficient for a hard sphere in a viscous medium.

It is important to note that the size determined by dynamic light scattering is the size of a sphere that moves in the same manner as the scatterer. So, for example, if the scatterer is a random coil polymer, the determined size is not the same as the <u>radius of gyration</u> determined by <u>static light scattering</u>.

It is also useful to point out that the obtained size will include any other molecules or solvent molecules that move with the particle. So, for example, <u>colloidal gold</u> with a layer of surfactant will appear larger by dynamic light scattering (which includes the surfactant layer) than by <u>transmission electron microscopy</u> (which does not "see" the layer due to poor contrast).

In most cases, samples are polydisperse. Thus, the autocorrelation function is a sum of the exponential decays corresponding to each of the species in the population.
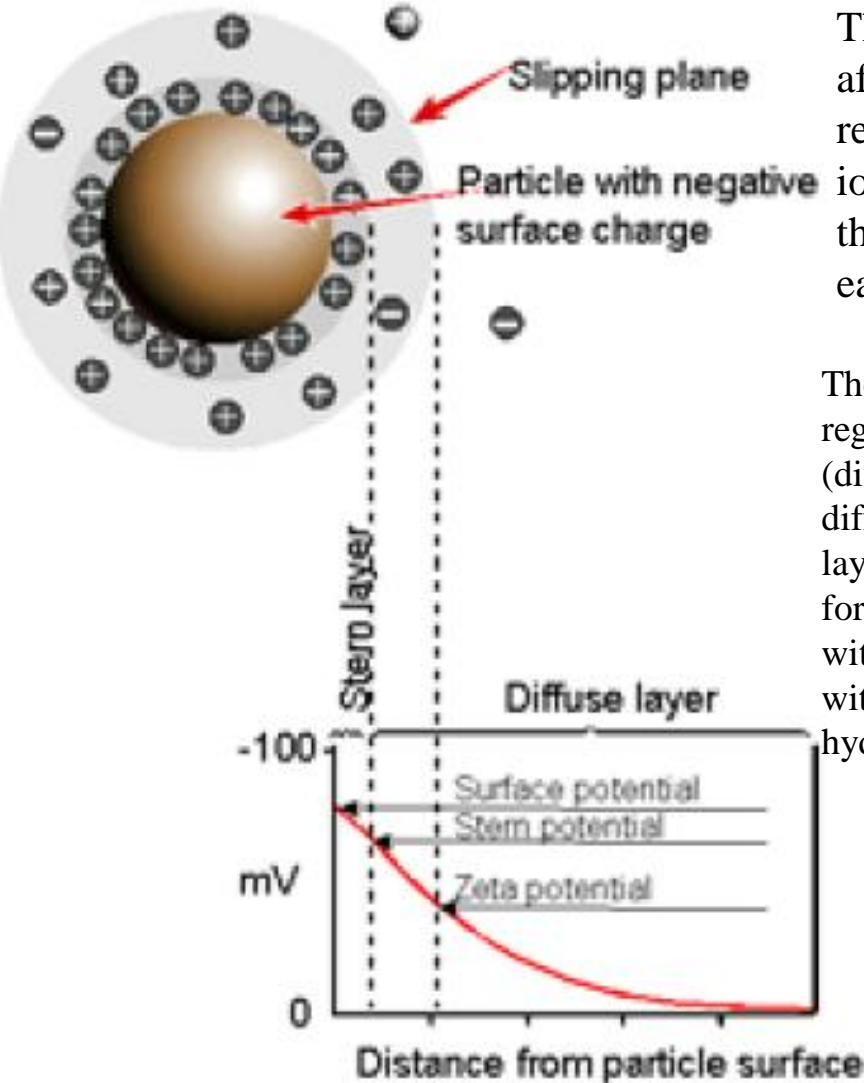
$$g^1(q;\tau) = \sum_{i=1}^{n} G_i(\Gamma_i)\exp(-\Gamma_i\tau) = \int G(\Gamma)\exp(-\Gamma\tau)\,d\Gamma.$$

From data for $g^1(q;\tau)$ one can extract $G(\Gamma)$. Since $G(\Gamma)$ is proportional to the relative scattering from each species, it contains information on the distribution of sizes.

DLS is used to characterize size of various particles including proteins, polymers, micelles, carbohydrates, and nanoparticles. If the system is monodisperse, the mean effective diameter of the particles can be determined. This measurement depends on the size of the particle core, the size of surface structures, particle concentration, and the type of ions in the medium.

Since DLS essentially measures fluctuations in scattered light intensity due to diffusing particles, the diffusion coefficient of the particles can be determined. DLS software of commercial instruments typically displays the particle population at different diameters. If the system is monodisperse, there should only be one population, whereas a polydisperse system would show multiple particle populations.

Zeta potential: the electrostatic potential at the slipping plane (shear plane)calculated from the electrophoretic mobility

Slipping plane

Particle with negative surface charge

Stern layer

Diffuse layer

-100

mV

0

Surface potential
Stern potential
Zeta potential

Distance from particle surface

The development of a net charge at the particle surface affects the distribution of ions in the surrounding interfacial region, resulting in an increased concentration of counter ions, ions of opposite charge to that of the particle, close to the surface. Thus an electrical double layer exists round each particle.

The liquid layer surrounding the particle exists as two parts; an inner region (Stern layer) where the ions are strongly bound and an outer (diffuse) region where they are less firmly associated. Within the diffuse
layer there is a notional boundary inside which the ions and particles form a stable entity. When a particle moves (e.g. due to gravity), ions within the boundary move with it. Those ions beyond the boundary stay with the bulk dispersant. The potential at this boundary (surface of hydrodynamic shear) is the zeta potential.

If all the particles in suspension have a large negative or positive zeta potential then they will tend to repel each other and there will be no tendency for the particles to come together.

Alguns exemplos de estabilidade e instabilidade coloidal

Importância do DLS para avaliar estabilidade coloidal

Combining all colloids to get biomimetic particles:
lipids and biomolecules on particles

lipid-covered particles
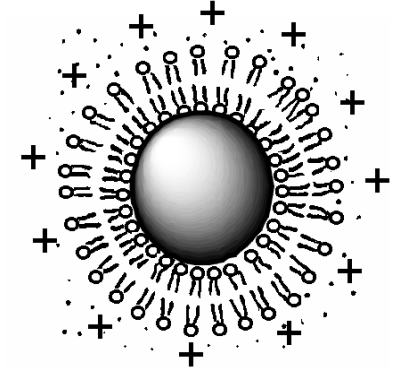
protein –lipid on particles

silica surface

Carmona-Ribeiro;
Midmore
Langmuir (**1992**), 8(3),
801-6.

Carmona-Ribeiro;
Herrington
J. Colloid Interface Sci.
(**1993**), 156(1), 19-23.
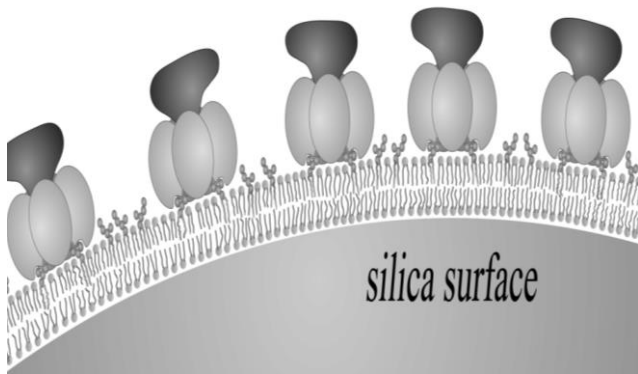
Moura; Carmona-Ribeiro,
Cell Biochemistry and Biophysics (**2006**), 44(3),
446-452.
Moura, S. P.; Carmona-Ribeiro, A M.
Langmuir (**2005**), 21(22), 10160-10164

Biomimetic Particles: nucleic acids on top

DNA on particles: nucleosome mimetic particles
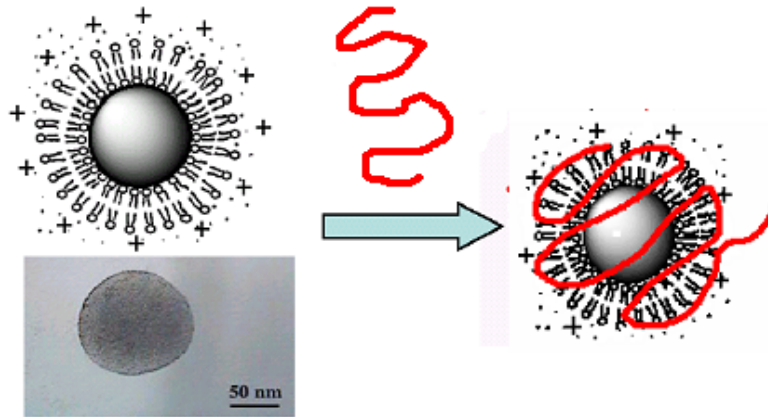
PSS137/DODAB/T2-DNA at charge neutralization
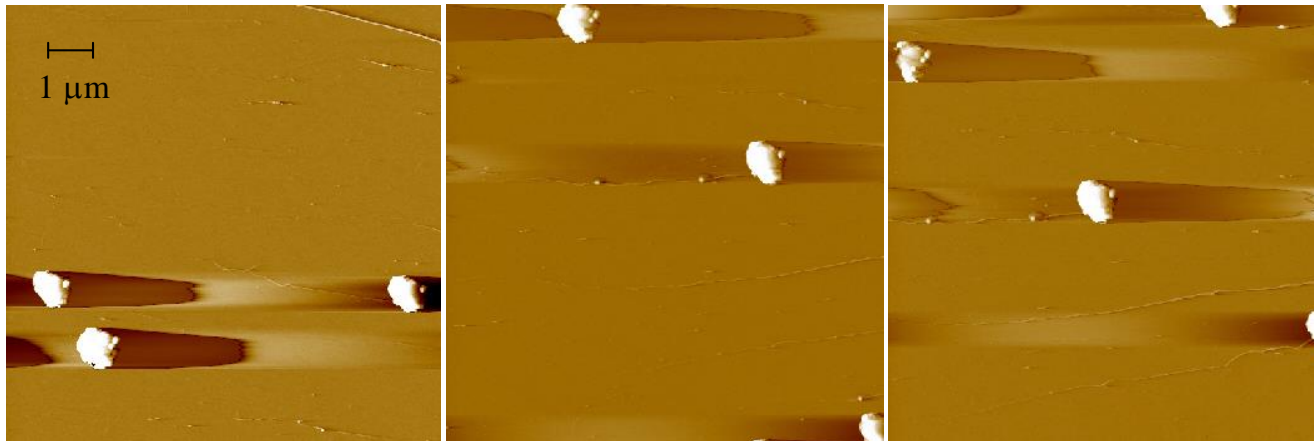
Cationic bilayer fragments on top of silica particles: colloidal stability from equivalence of total surface area for bilayers and particles

$$A_{bilayer}/A_{particles}=1$$

KCl concentration / mM

10.0
1.0
0.5
0.1
0

0 0.2 0.3 0.7 1.0 1.7 2.0 3.5

A_b / A_s
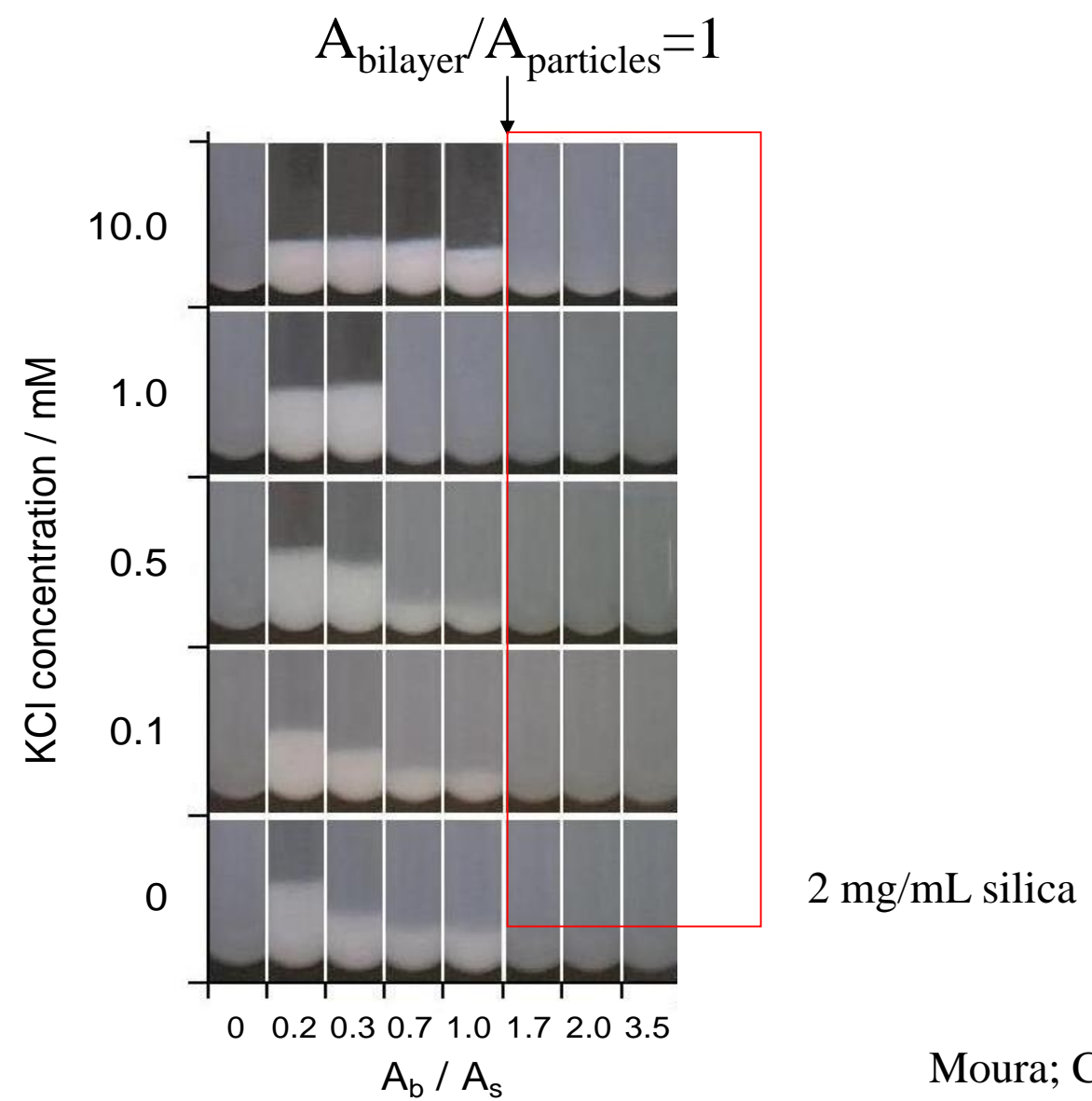
2 mg/mL silica

Moura; Carmona-Ribeiro, *Langmuir* 2003, 19, 6664.

Antigens on top: 0.05 mM of cationic lipid covers 0.1 mg/mL silica with a cationic bilayer prone to adsorb antigens

Lincopan et al. BMC Biotechnology (2009) 9: article 5
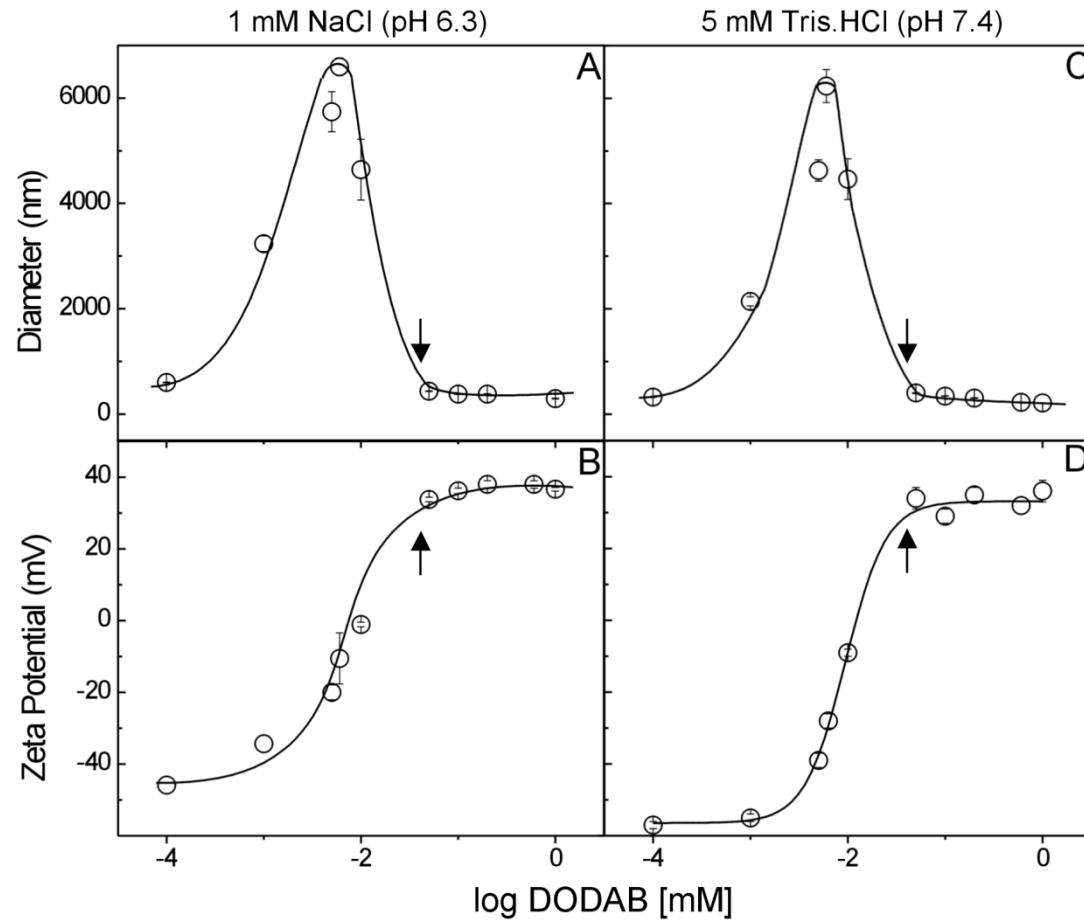
Polymeric particles and cationic bilayer on top
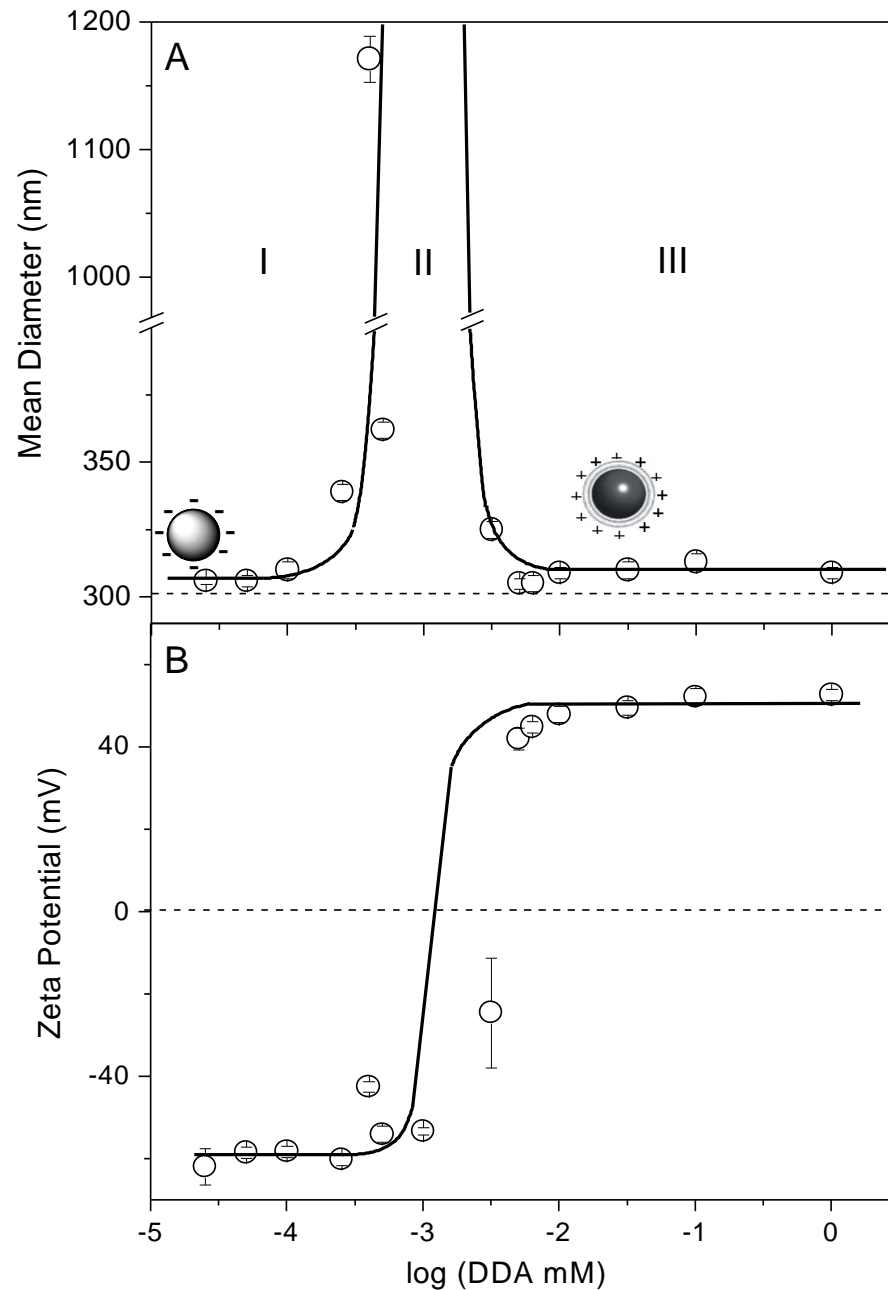
1 mM NaCl

Biomolecules on top of cationic supported bilayers

biomolecules

50 nm
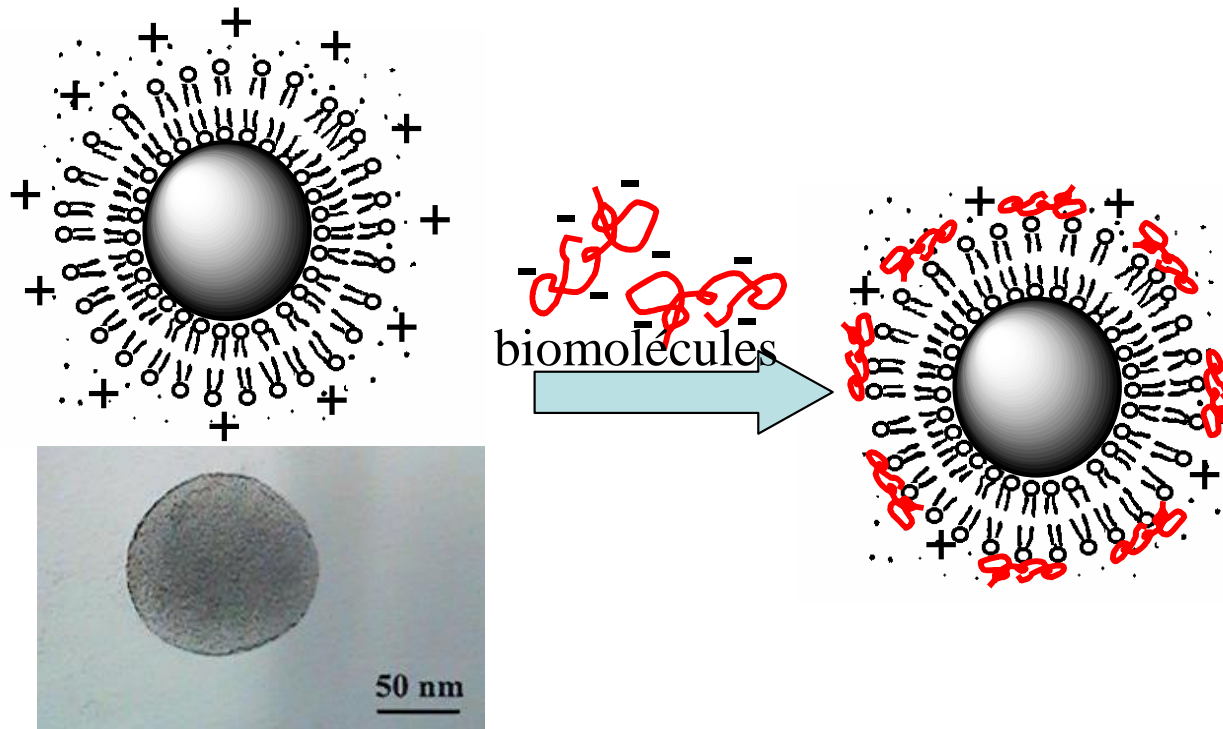
Adsorption of antigen onto cationic supported bilayers

Lincopan et al. Int. J. Pharm.(2007) 340, 216
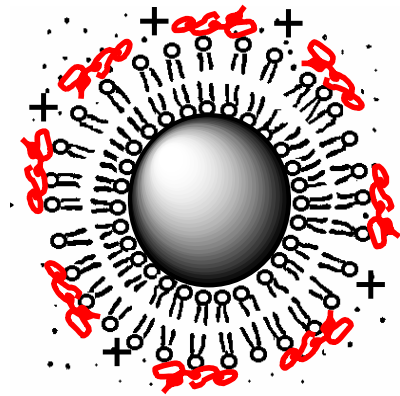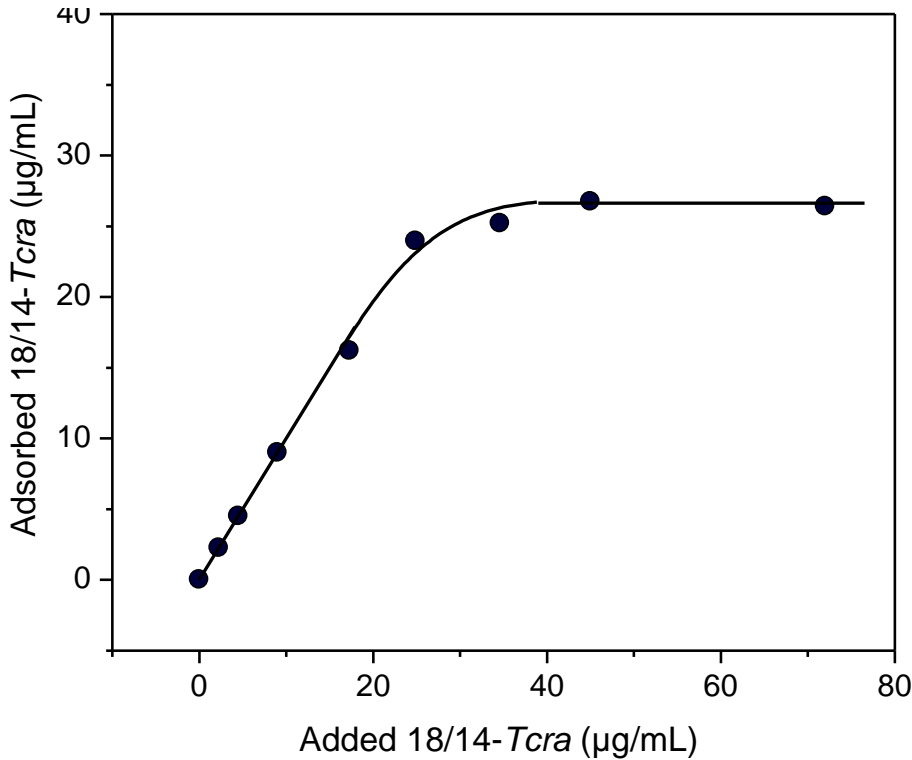
Narrow size distribution for antigen adsorbed onto supported cationic bilayers from dynamic light scattering

A

229

18/14-*Tcra* 25 μg/mL

D_z = 310 ± 5 nm
ζ = -52 ± 1 mV

B

385

DDA/18/14-*Tcra* 25 μg/mL

D_z = 295 ± 3 nm
ζ = 6 ± 6 mV

C

309

PSS/DDA/
18-14/*Tcra* 5 μg/mL

D_z = 316 ± 2 nm
ζ = 25 ± 6 mV

D

328

PSS/DDA/
18-14/*Tcra* 25 μg/mL

D_z = 328 ± 3 nm
ζ = 11 ± 8 mV
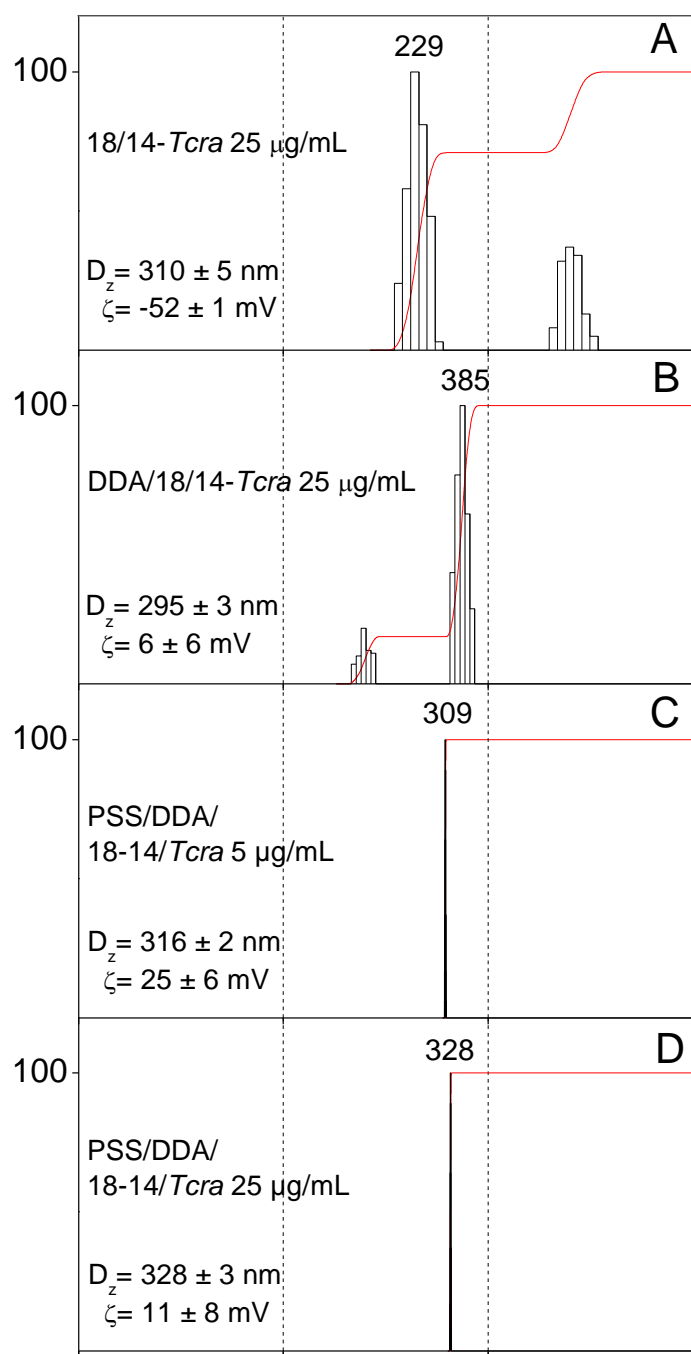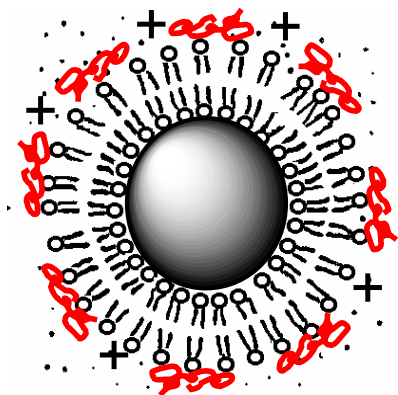
Biomimetic particles: artificial viruses?
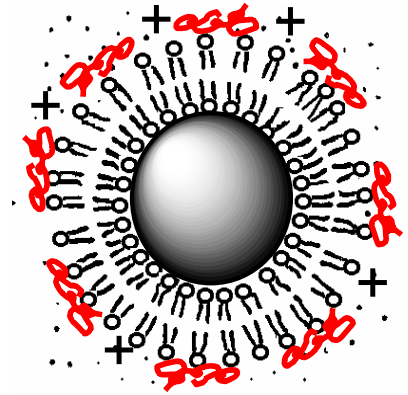
Sample	DDA (μM)	Ag (μg/mL)	Mean diameter (nm)	Zeta-Potential (mV)	Polydispersity index
PSS	-	-	301 ± 2	- 60 ± 1	0.064 ± 0.020
DDA	2,000	-	81 ± 1	45 ± 2	0.230 ± 0.006
PSS/DDA	7	-	309 ± 2	48 ± 2	0.040 ± 0.010
PSS/DDA/18/14-*Tcra*	7	25	328 ± 3	11 ± 8	0.060 ± 0.020

Drug particles covered by oppositely charged bilayer disks: synergism in certain cases

Vieira, DB.; Pacheco, LF.; Carmona-Ribeiro, A M.
J. Colloid Interface Sci. **2006** 293, 240.

Lincopan, N.; Carmona-Ribeiro, A M
J. Antimicrobial Chemother. **2006**, 58, 66.
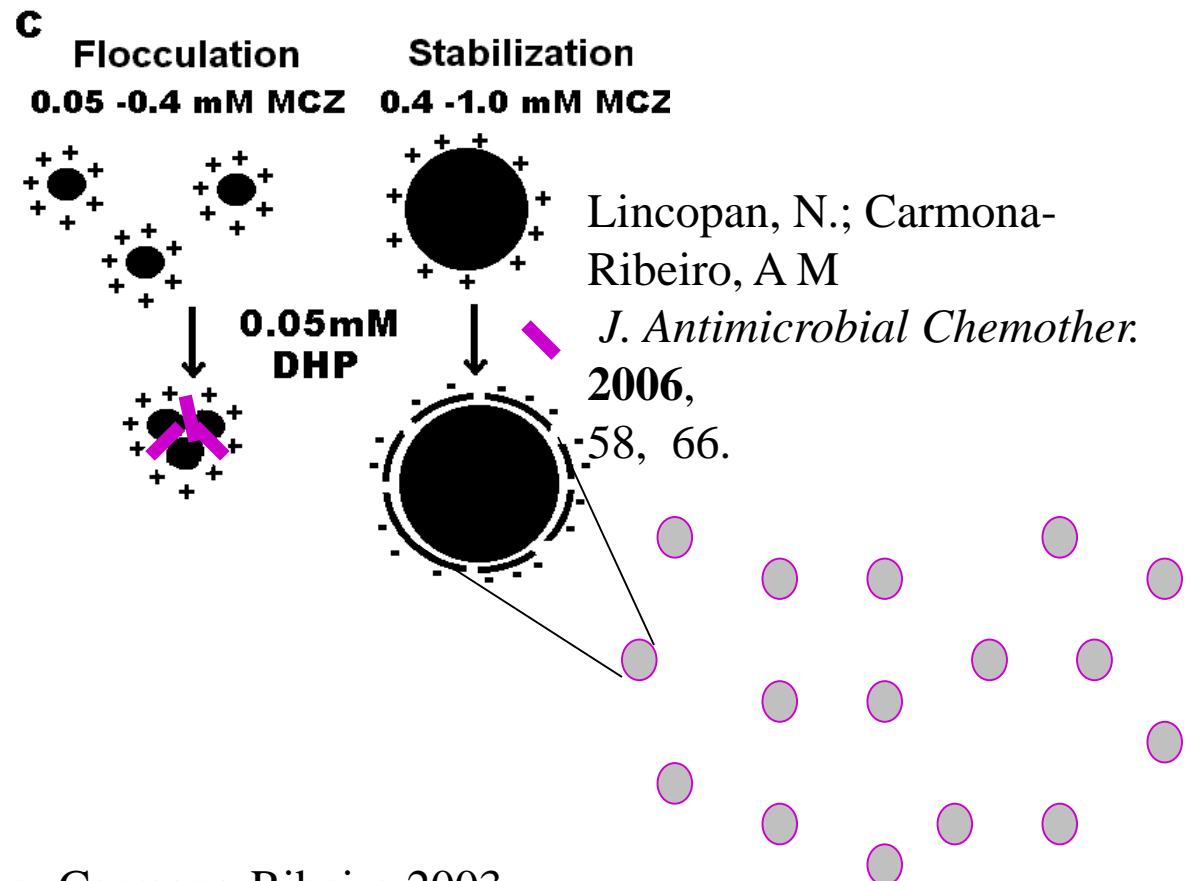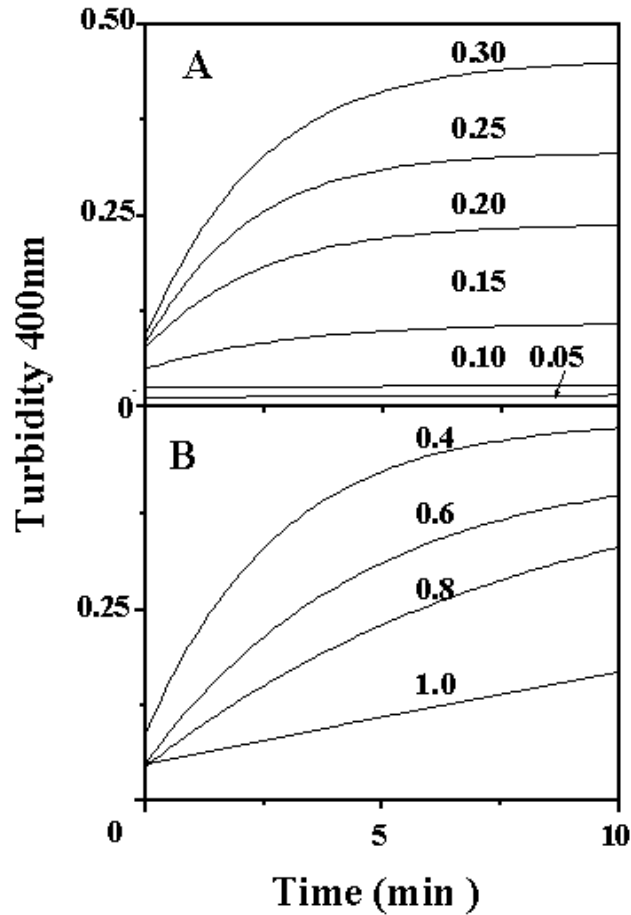
Pacheco; Carmona-Ribeiro 2003
J. Colloid Interface Sci. 258,146.

Fungicidal formulation from amphotericin B/cationic lipid/polyelectrolytes
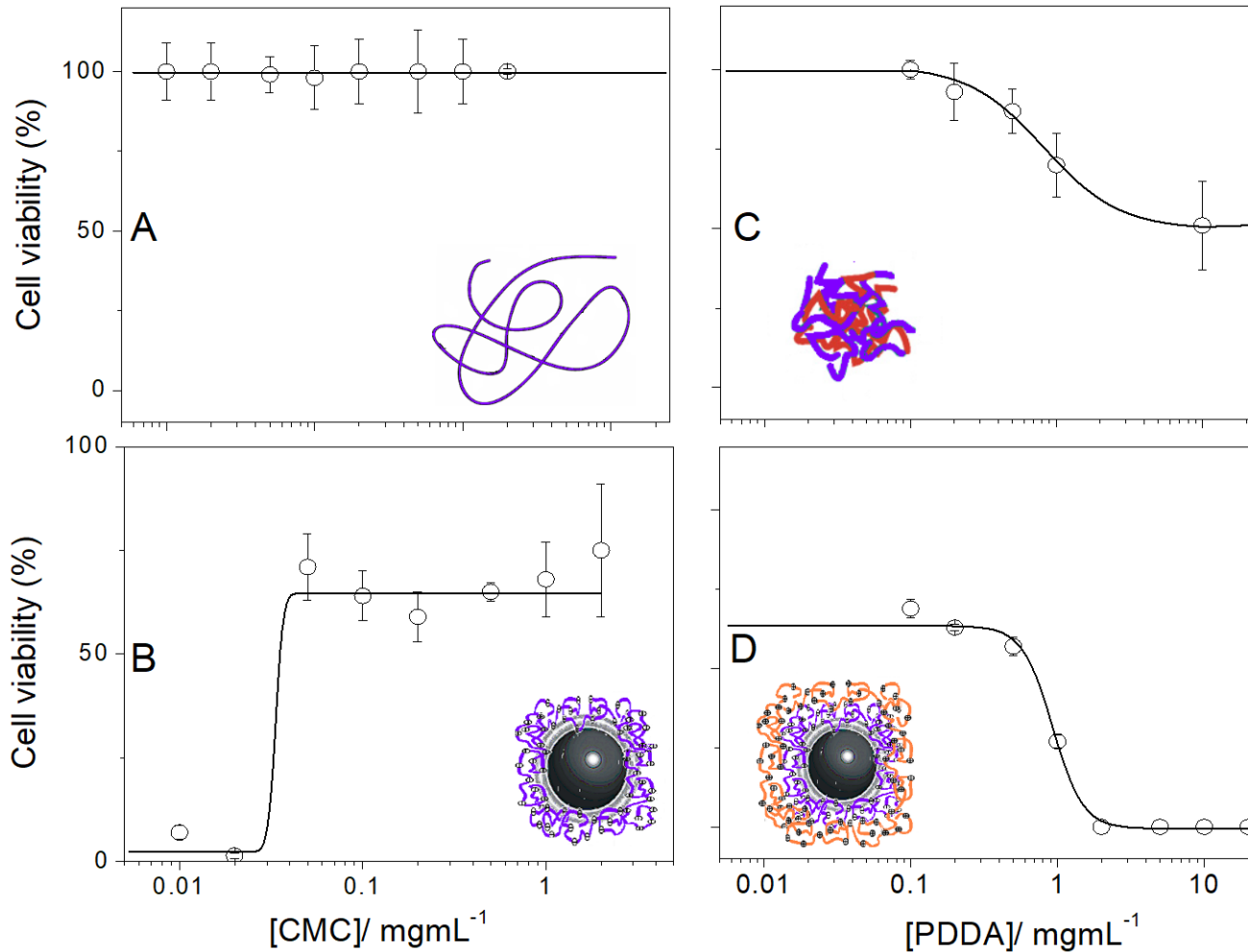
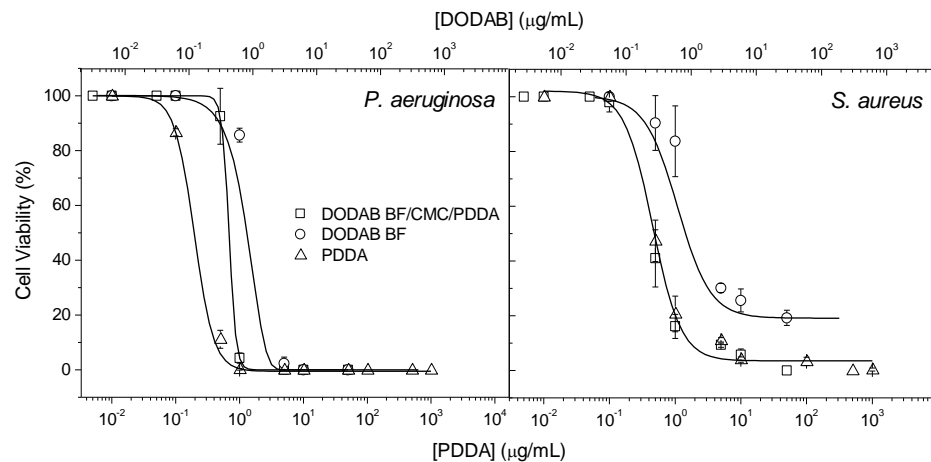*Candida albicans*

Antimicrobial particles from cationic lipid and polyelectrolytes
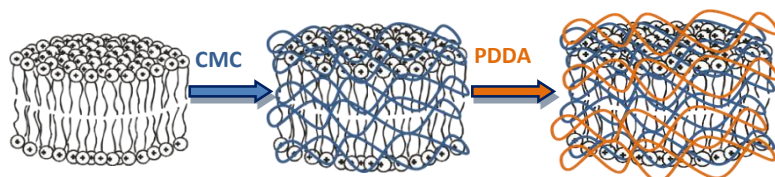
Assembly	[DODAB] mg/mL	mM	[CMC] mg/mL	[PDDA] mg/mL
Small particles Dz=100nm ζ=30 mV	0.06	0.1	0.100	0.100
Large particles Dz=470 nm ζ=50 mV	0.32	0.5	0.500	0.500

Small particles

Large particles

Melo, L.D.; Mamizuka, E.M.; Carmona-Ribeiro, A.M. Langmuir (2010) 26,12300.
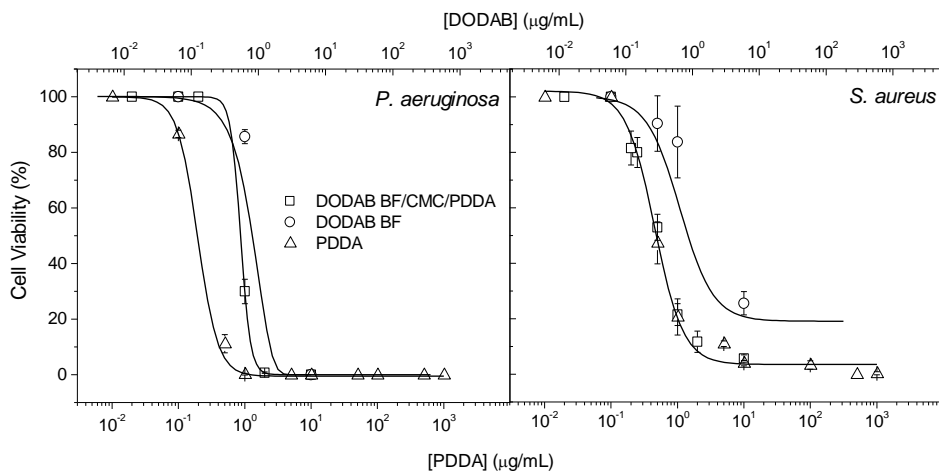
Antimicrobial particles from emulsion polimerization of methacrylic acid in the presence of quaternary ammonium surfactants or lipids

Gram-negative Rods

+

Gram-positive Cocci

PMMA/CTAB or PMMA/DODAB NPs

Bacterial death
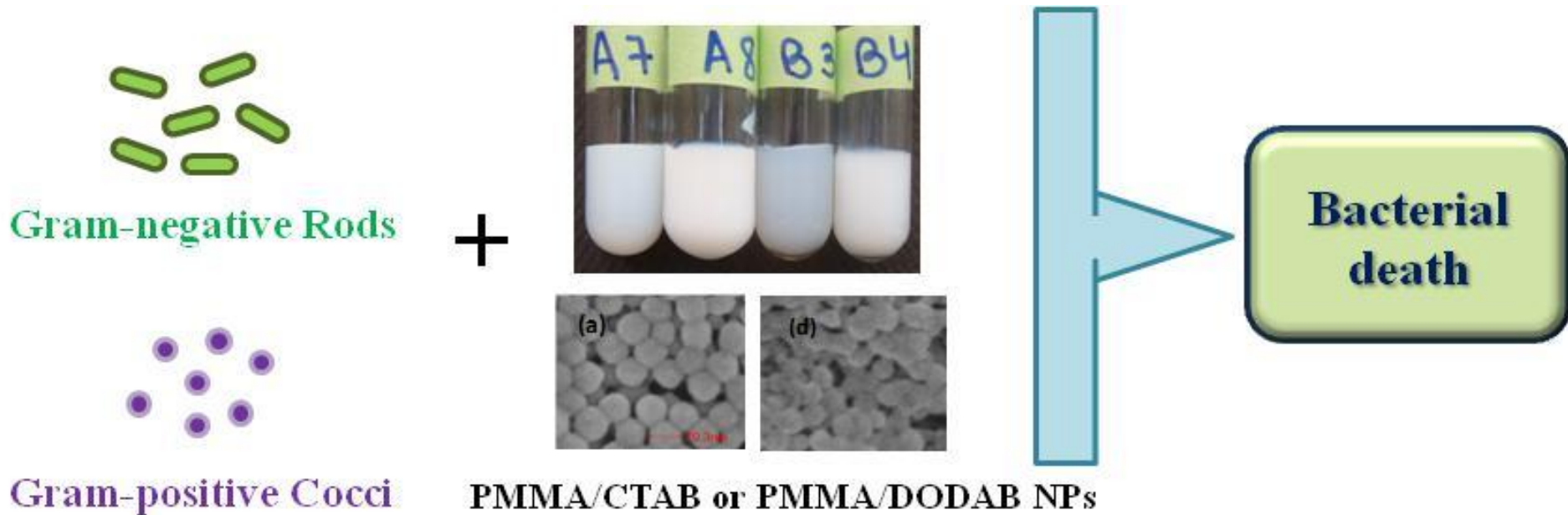
A.F. Naves, R. R. Palombo, L. D. M. Carrasco, A. M. Carmona-Ribeiro (2013) Langmuir 29(31), 9677-9684.

Supramolecular assemblies of cationic bilayer fragments and polyelectrolytes are active against multidrug resistant microorganisms
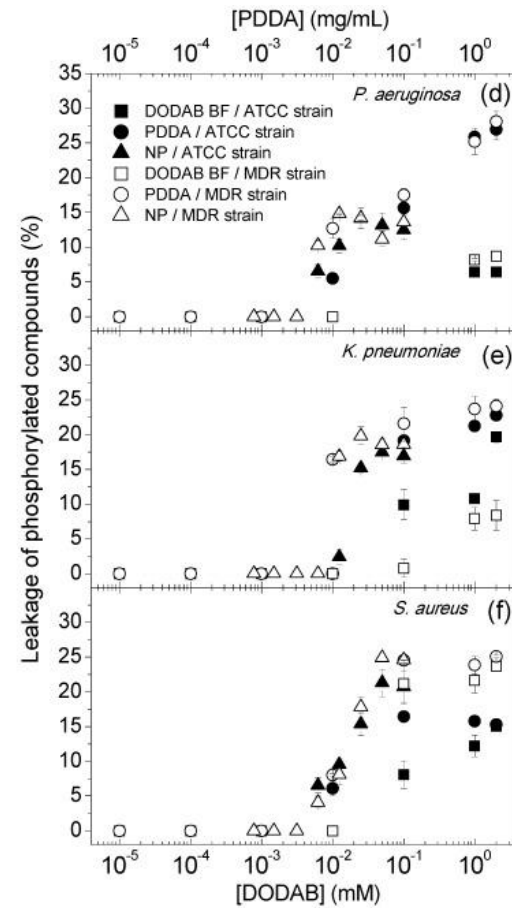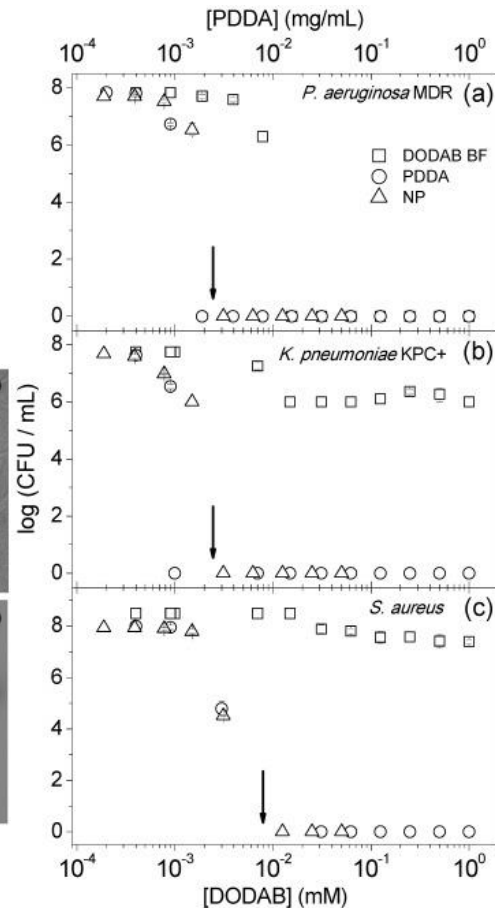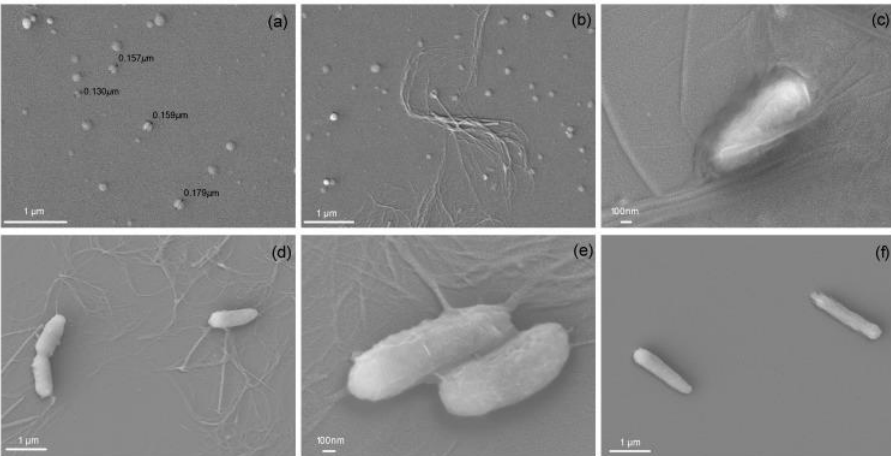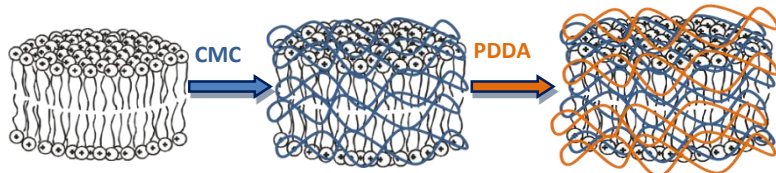

Carrasco LD, Sampaio JL, Carmona-Ribeiro AM.
Supramolecular cationic assemblies against multidrug-resistant microorganisms: activity and mechanism of action.
Int J Mol Sci. 2015 Mar 19;16(3):6337-52.

Assemblies from cationic lipid and non-steroidal anti-inflammatory drugs in the presence of a co-solvent form stable NPs in dispersions containing anionic biopolymer
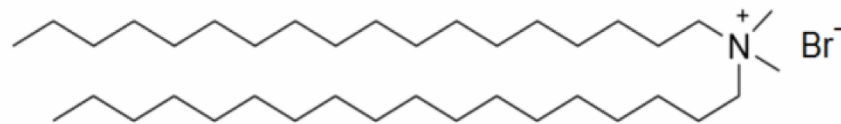

stable cationic NPs

anionic biopolymer

stable anionic NPs
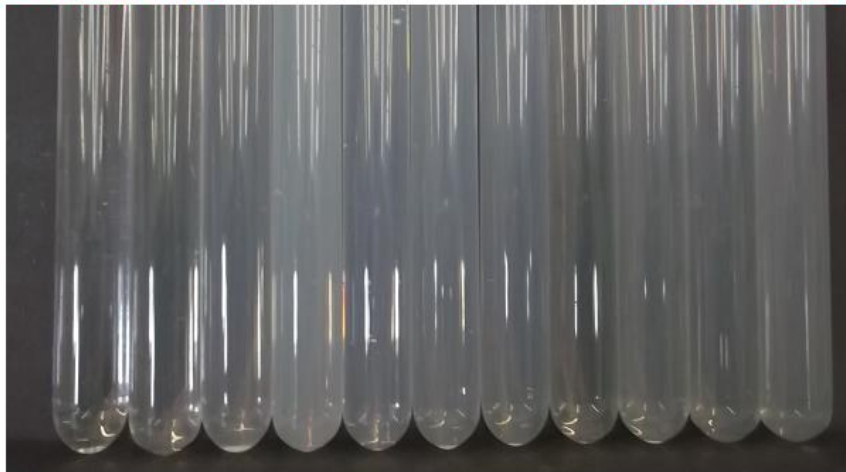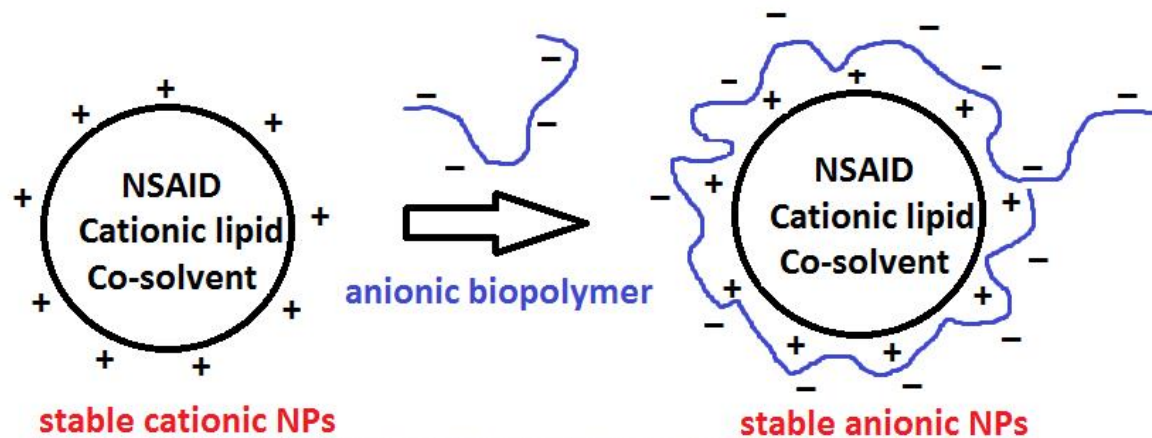
Stable indomethacin dispersions in water from drug, ethanol, cationic lipid and carboxymethyl–cellulose
Lima EG, Gomes LR, Carmona-Ribeiro AM
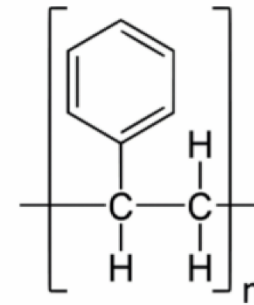Pharmaceutical Nanotechnology, 2016 , 4, 126-135.

Combining the antimicrobial peptide gramicidin, nanoparticles and cationic bilayers
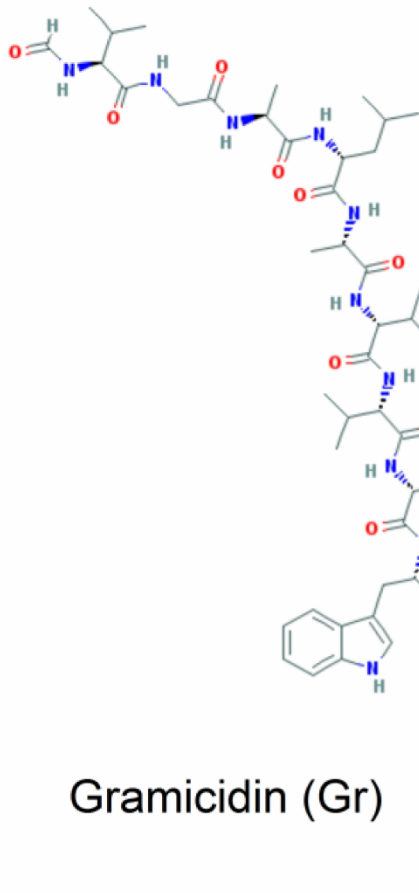
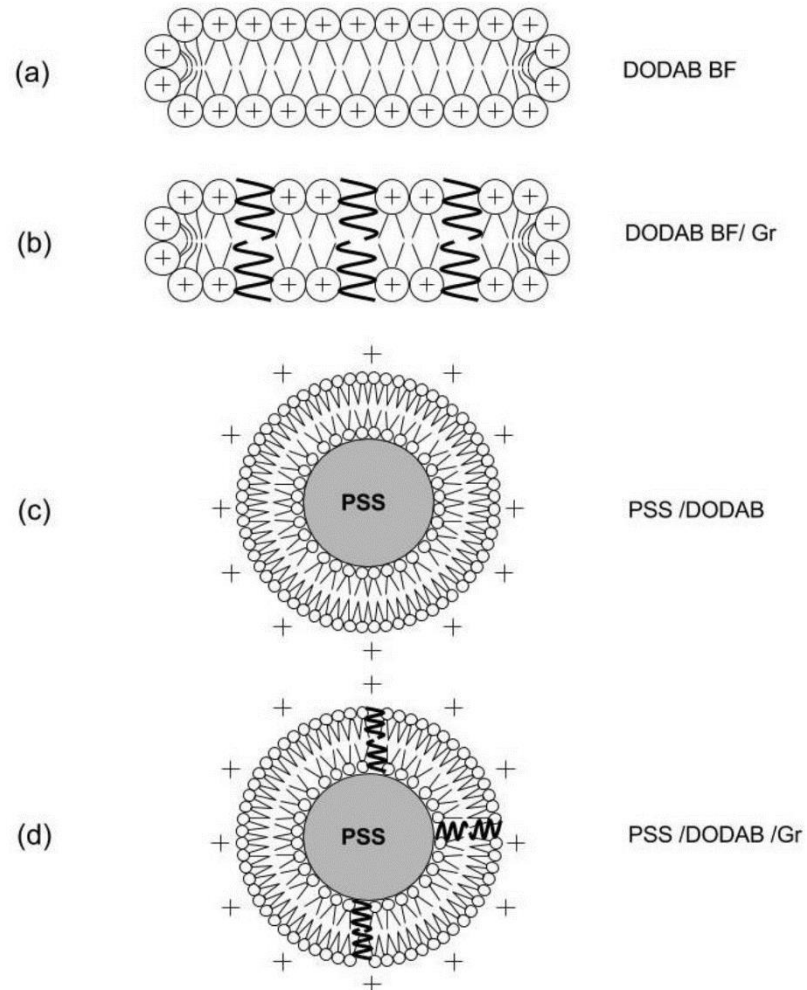Dioctadecyldimethylammonium bromide (DODAB)

Polystyrene (PSS)
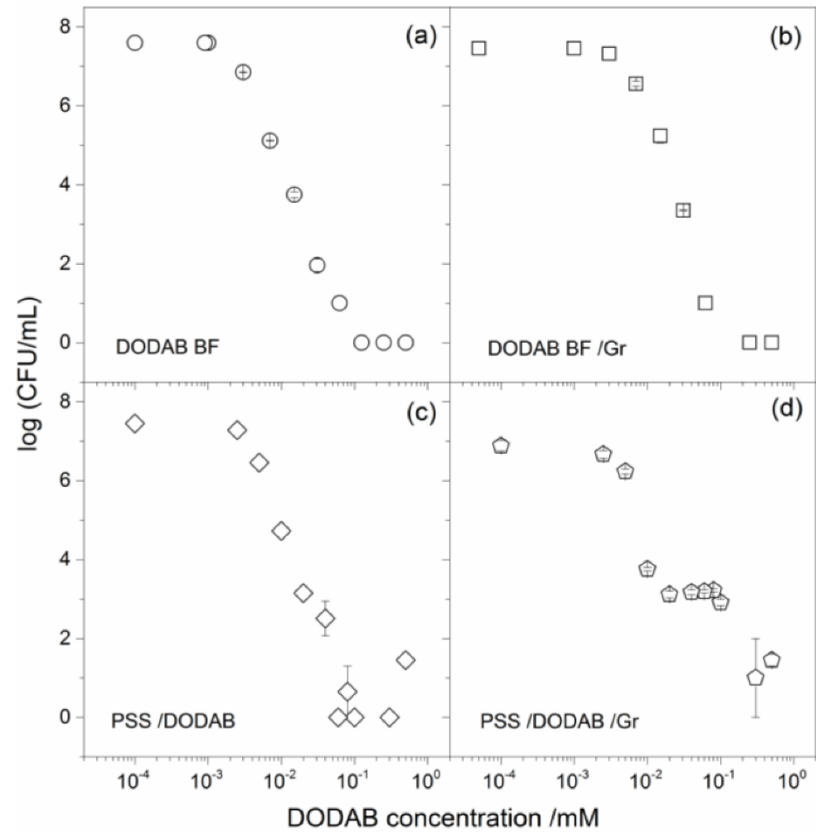
Gramicidin (Gr)

Supported cationic bilayers for functional peptide helix

(a) DODAB BF

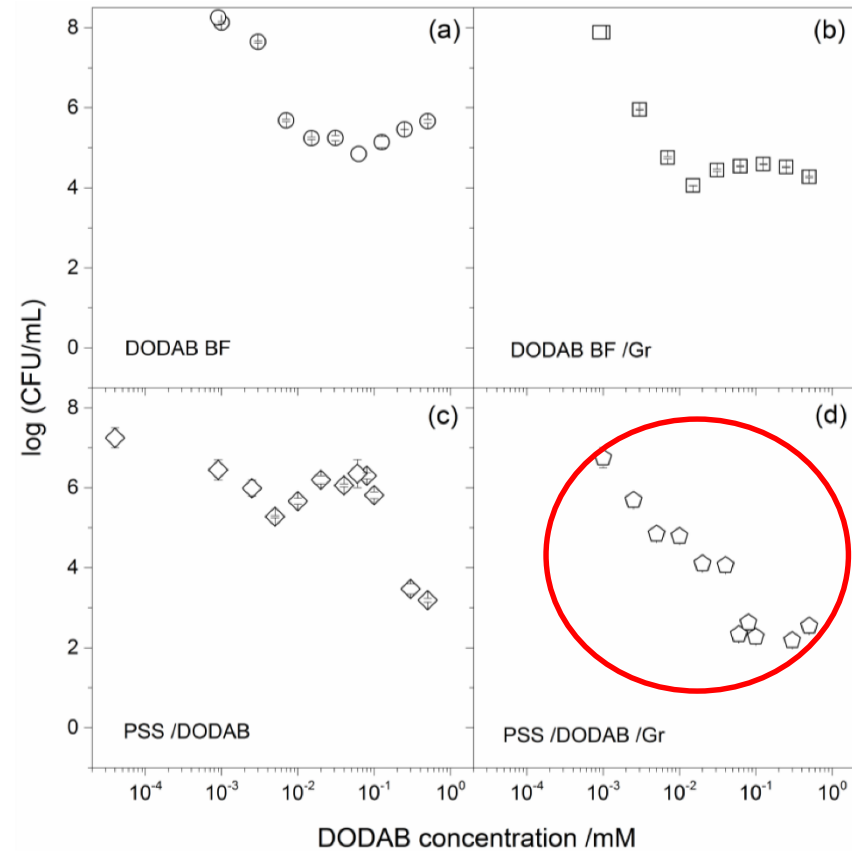(b) DODAB BF/ Gr

(c) PSS /DODAB

(d) PSS /DODAB /Gr

Combined activity against *E. coli* and *S. aureus*

E. coli

S. aureus

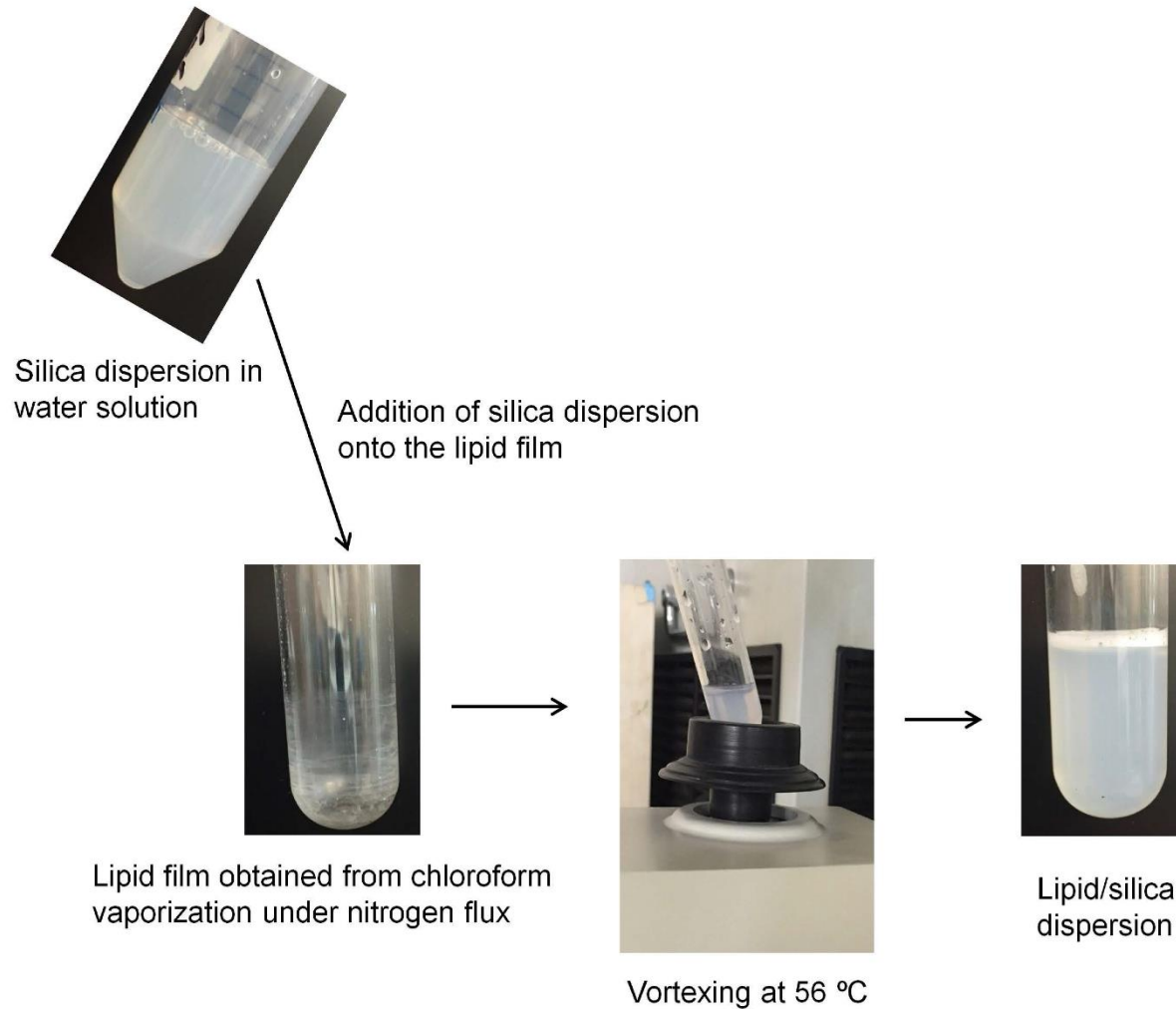Xavier and Carmona-Ribeiro (2017)Cationic Biomimetic Particles of Polystyrene/Cationic Bilayer/Gramicidin for Optimal Bactericidal Activity. **Nanomaterials** 7, 422
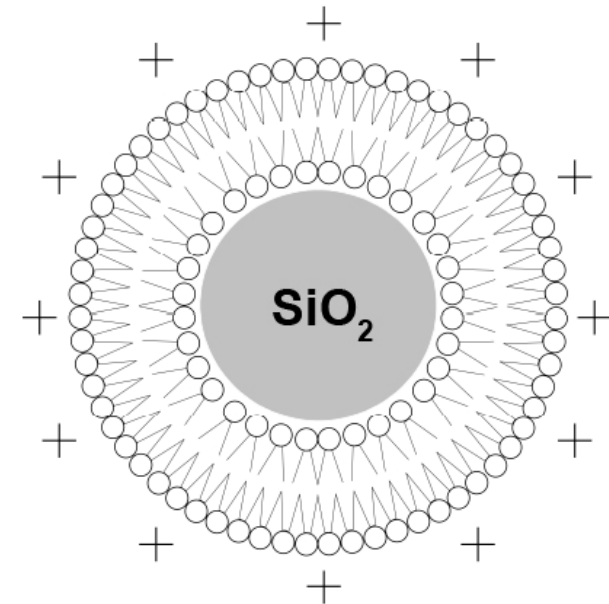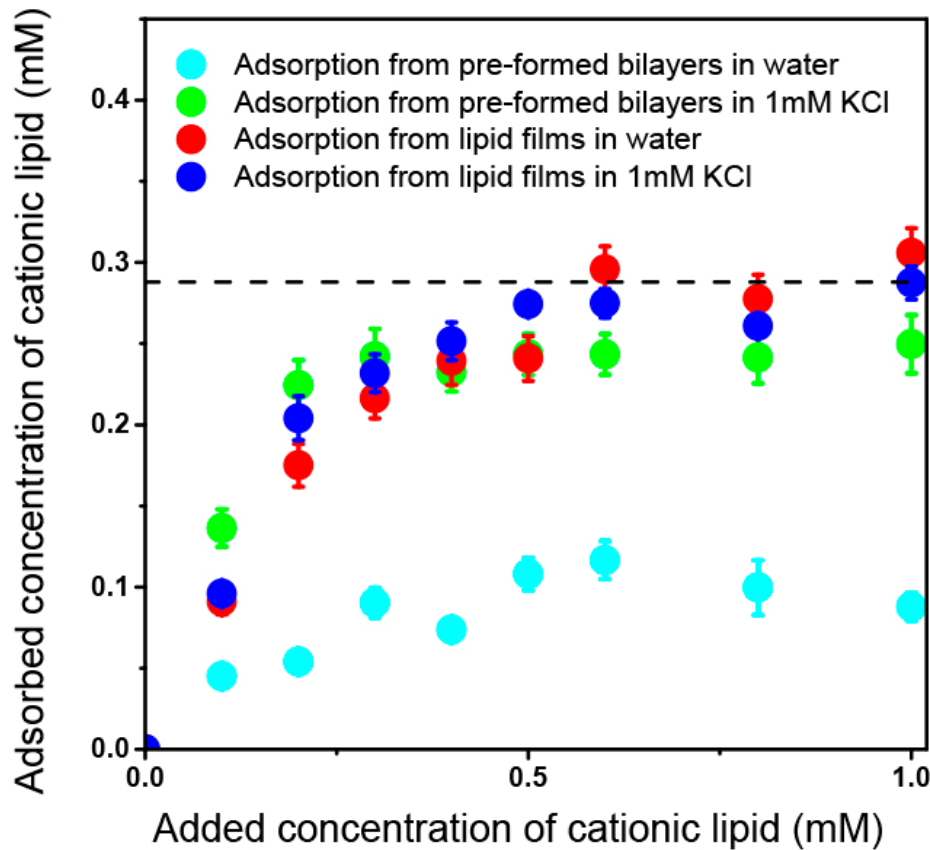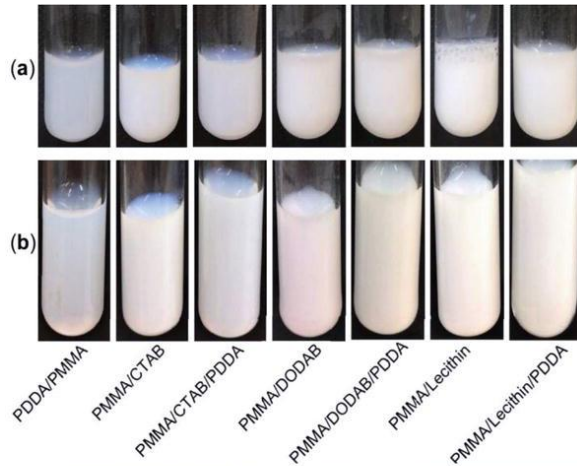
Optimizing cationic lipid adsorption onto silica nanoparticles: using lipid films

Silica dispersion in water solution

Addition of silica dispersion onto the lipid film

Lipid film obtained from chloroform vaporization under nitrogen flux

Vortexing at 56 ºC

Lipid/silica dispersion

Bilayer adsorption from lipid films instead pre-formed bilayers

Ribeiro, R.T.; Braga, V.H.A.; Carmona-Ribeiro, A.M. Biomimetic Cationic Nanoparticles Based on Silica: Optimizing Bilayer Deposition from Lipid Films. *Biomimetics* **2017**, *2*, 20

Antimicrobial dispersions and coatings

(a)

(b)

PDDA/PMMA   PMMA/CTAB   PMMA/CTAB/PDDA   PMMA/DODAB   PMMA/DODAB/PDDA   PMMA/Lecithin   PMMA/Lecithin/PDDA

The dispersions

(c)

The coatings

(d)
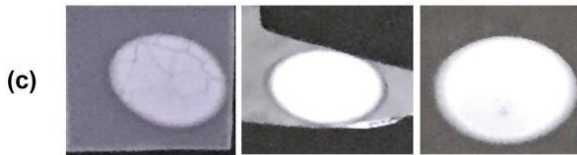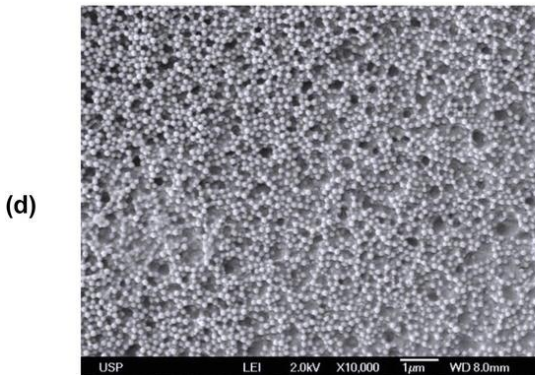
The coatings from nanoparticles casted from dispersions

Galvão, C.N.; Sanches, L.M.; Mathiazzi, B.I.; Ribeiro, R.T.; Petri, D.F.S.; Carmona-Ribeiro, A.M. Antimicrobial Coatings from Hybrid Nanoparticles of Biocompatible and Antimicrobial Polymers. *Int. J. Mol. Sci.* **2018**, *19*, 2965